PAPER

Check for updates

Water–rock interaction and the concentrations of major, trace, and rare earth elements in hydrocarbon-associated produced waters of the United States†

Carleton R. Bern, [ID] *[a] Justin E. Birdwell [ID] [b] and Aaron M. Jubb [ID] [c]

Studies of co-produced waters from hydrocarbon extraction across multiple energy-producing basins have generally focused on major ions or a few select tracers, and studies that examine trace elements and involve laboratory experiments have generally been basin specific. Here, new perspective is sought through a broad analysis of concentration data for 26 elements from three hydrocarbon well types using the U.S. Geological Survey National Produced Waters Geochemical Database (v2.3). Those data are compared to leachates (water, hydrochloric acid, and artificial brine) from 12 energy-resource related shales from across the United States. Both lower pH and higher ionic strength were associated with greater concentrations of many trace elements in produced waters. However, individual effects were difficult to distinguish because higher ionic strengths drive decreases in pH. Water–rock interactions in the leaching experiments generally replicated produced water concentrations for trace elements including Al, As, Cd, Co, Cu, Mo, Ni, Pb, Sb, Si, and Zn. Enhanced middle rare earth element (REE) mobilization relative to shale REE content occurred with low pH leachates. Produced water concentrations of Li, Sr, and Ba were not replicated by the leaching experiments. Patterns of high Li, Sr, and Ba concentrations and ratios relative to other elements across produced waters types indicate controls on these elements in many settings related to pore space pools of salts, brines, and ion-exchange sites affected by diagenetic processes. The size of those pools is diluted and masked by other water–rock interaction processes at the water–rock ratios necessitated by laboratory experiments. The results broadly link water–rock interaction processes and environmental patterns across a wide variety of produced waters and host formations and thus provide context for trace element data from other environmental and laboratory studies of such waters.

Environmental significance statement

Management and disposal of waters co-produced with oil and natural gas development pose a challenge because of their chemistry. Multi-basin comparisons of such produced waters have generally focused on a few major constituents due to data availability. Studies incorporating trace element data and laboratory experiments to replicate water–rock interaction have generally focused on single basins. The present study bridges those two viewpoints. Comparisons of produced waters from multiple basins in the United States and water–rock interaction experiments using multiple hydrocarbon-associated shales provide useful perspective on both typical elemental concentrations and the water–rock interactions that influence them.

[a]U.S. Geological Survey, Colorado Water Science Center, Denver, Colorado, USA. E-mail: cbern@usgs.gov

[b]U.S. Geological Survey, Central Energy Resources Science Center, Denver, Colorado, USA

[c]U.S. Geological Survey, Geology, Energy & Minerals Science Center, Reston, Virginia, USA

† Electronic supplementary information (ESI) available: Additional details on analyses of bulk shale and leachates (Section S1). Table summaries of statistics from PWGD data (Tables S1–S8), bulk shale mineralogy and carbon characteristics (Tables S9 and S10), fractions of elements extracted from shales and correlations with leachate pH (Table S11). Figures depicting basin median concentrations of TDS and values of pH (Fig. S1), basin median concentrations of Na and Cl (Fig. S2), relations between Cl and selected major elements in produced waters (Fig. S3), relations between pH and selected major elements in produced waters (Fig. S4), shale compositions normalized to reference compositions (Fig. S5), relations between REEs and other elements in HCl leachates (Fig. S6), relations between REEs in HCl leachates and illite in shale (Fig. S7), and relations between SO_4^{2-} in produced waters and Ca, Sr, and Ba (Fig. S8). See DOI: 10.1039/d1em00080b

1198 | *Environ. Sci.: Processes Impacts*, 2021, **23**, 1198–1219

This journal is © The Royal Society of Chemistry 2021

1. Introduction

The potential for waters associated with developed hydrocarbon reservoirs to migrate through the subsurface or be released into the surface environment and affect potable water supplies or environmental quality more generally has generated public concern.[1–5] Although conventional hydrocarbon development also co-produces water, the large volumes of high-salinity brine extracted during oil and gas production from resources termed unconventional, continuous, or "shale plays" over the last 10+ years have become a key factor in the public's perspective regarding the development of these resources.[6,7] Rapid expansion of unconventional resource development has been possible because of directional or horizontal drilling and hydraulic fracturing that increases the surface area contact between reservoir rocks and fluid flow paths to more efficiently liberate hydrocarbons and associated fluids from low permeability rock matrices.[8] The concern over co-produced waters from shale resource development has led to research related to the characterization, disposal, potential reuse, and co-product development potential of produced waters.[9–12]

From all perspectives, understanding the composition of produced waters is crucial. The two major controls on produced waters' composition are generally considered to be (1) inheritance from connate and more freely circulating water within the rock matrix and attributed to paleo-seawater from around the time of deposition, seawater-derived evaporites and bitterns, and younger meteoric water, and (2) water–rock interactions with both mineral and organic matter that lead to a dynamic equilibrium that evolves slowly as the rocks and waters experience changing thermal stress during burial and uplift, and more rapidly in response to development-related disturbance.[13–17] A sub-category of produced waters is flowback water, which is a mixture dominated by fluids injected during hydraulic fracturing that return to the surface days or weeks after injection. Over time, the chemical composition of flowback waters shift towards that of formation waters from which they cannot be precisely distinguished.[18–21]

In addition to direct characterization, other studies have taken an experimental approach to understanding the compositions of produced waters. Leaching or elemental mobilization studies use source and reservoir rocks from one or more systems and expose them to aqueous media under conditions meant to mimic reservoir or well environments (e.g., elevated temperature and pressure). Such studies focus on the water–rock interaction component of produced waters compositions, or how hydraulic fracturing fluids can mobilize or precipitate elements from the rock matrix, but often fail to reproduce concentrations observed in actual produced waters.[22–28]

Broad studies of produced waters encompassing multiple energy-producing basins have generally focused on patterns in a few, often major, elements because of data availability.[21,29] In contrast, studies examining suites of trace elements and water–rock interaction experiments have typically focused on shales from one or two basins.[25–27,30–33] The present study seeks to bridge those viewpoints.

The objectives of this work were to better understand controls on water–rock interactions and how they influence the concentrations of 26 elements in produced waters from energy producing basins across the United States. Two types of data were drawn upon. First were data from the U.S. Geological Survey (USGS) National Produced Waters Geochemical Database (PWGD) which includes water compositions from various types of hydrocarbon-producing formations.[34] Second were data from 3 leaching experiments using 12 shales from active hydrocarbon resource plays across the United States covering a range of mineralogy and including immature (marine and lacustrine) and thermally mature source rocks.[35–37] The different leachates allowed comparison of effects of low ionic strength (deionized water), high ionic strength (artificial brine), and low pH (HCl) on water–rock interactions. In addition to the major and trace elements, rare earth element (REE) concentrations in shales and shale leachates were also evaluated as their patterns in produced waters have received little study.[38,39]

The results are evaluated from several perspectives: (1) understanding typical concentrations of major and trace elements in produced waters by comparisons within and between basins (2) understanding which elements are more influenced by water–rock interaction than inheritance from seawater and its derivatives (3) understanding the influences of fluid chemistry (pH and ionic strength) and shale mineralogy on water–rock interaction, and (4) understanding how simple water–rock interaction experiments do and do not replicate compositions of produced waters. Patterns and processes elucidated here provide useful perspective on both water–rock interaction and the concentrations of major, trace, and rare earth elements in hydrocarbon-associated produced waters of the United States and elsewhere.

2. Materials and methods

2.1 USGS national produced waters geochemical database v2.3

The most extensive compilation of major and trace element concentrations in produced waters from across the United States is the USGS PWGD (v2.3), which contains data for 114 943 individual samples of produced waters in its current iteration.[34] The database identified samples by well type, and data from the conventional hydrocarbon, shale gas, and tight oil categories were examined for this study. Here, concentrations were converted from ppm to mg L^{-1} where necessary by multiplying analyte concentration by the sample specific gravity. Condensate and early flowback waters are not flagged in the PWGD and often require operational or geochemical context to identify. To generally exclude samples that might be dilute condensate or early flowback waters, samples were culled if pH was outside the range of 4.5–10.5 or if total dissolved solids (TDS) were <5000 mg L^{-1}.[40] Remaining data were expected to represent samples with high proportions of formation water. The PWGD is a compilation of data from 40 databases, publications, and reports, many of which are compilations themselves, which makes data quality assessment challenging.[34] Analytical artifacts and quality issues may affect some of the data utilized

This journal is © The Royal Society of Chemistry 2021

Environ. Sci.: Processes Impacts, 2021, **23**, 1198–1219 | **1199**

here. However, the number of data sources reduces the influence of errors and artifacts from individual sources, and because of the broad scope of analysis presented, the resulting patterns are most likely not substantially affected by such errors.

2.2 Shale samples

The goal of the leachate experiments was to explore the ranges of potential trace element mobilization by water–rock interaction with shales. For this purpose, six thermally mature (*i.e.*, have generated hydrocarbons) and six thermally immature samples of energy resource related shales were used for the leachate experiments. The thermally mature samples included the Devonian Marcellus shale of the Hamilton Group, hereafter referred to as the Marcellus shale (New York; two samples), the Devonian to Mississippian Bakken formation (North Dakota), the Mississippian Barnett formation (Texas), the Cretaceous Niobrara formation of the Colorado Group, hereafter referred to as the Niobrara formation (Colorado), and the Paleogene Uteland Butte member (informal[41–43]) of the Green River formation (Utah). The thermally immature samples included the Devonian to Mississippian Woodford shale (Oklahoma), the Cretaceous Boquillas formation (Texas; Eagle Ford shale equivalent), the Cretaceous Mancos shale (Colorado), and the Paleogene Cow Ridge, Garden Gulch, and Parachute Creek Members of the Green River formation (Colorado). Additional details on the shale samples can be found in Croke *et al.* (2020).[37] These samples represent several extensively developed and highly productive shale resource plays in the United States for both oil (Woodford, Bakken, Niobrara, and Eagle Ford) and gas (Marcellus, Barnett) as well as less developed hydrocarbon systems with substantial potential (Mancos, Uteland Butte). Oil shales from the Green River formation in Colorado were included to represent non-marine, organic-matter rich lacustrine shales deposited under different lake conditions leading to mineralogical differences.[44] The samples represent most of the anticipated mineralogy range for hydrocarbon source rock types.[16]

2.3 Extractions and analytical methods

The 12 shales were hand crushed in a corundum mortar and pestle and sieved using stainless steel sieves. Material <500 μm was then powdered in an agate shatterbox to <75 μm prior to bulk elemental and mineralogical analysis. Complete details on shale rock analyses can be found in the ESI.†

Three different leachate extractions were conducted (water, HCl, brine), each in duplicate and using crushed shale (700–1000 μm) that was rinsed with deionized water to remove powdered material. Water leaches used 2.5 g of shale in 50 mL polytetrafluoroethylene (PTFE) digestion vessels. Prior to leaching, the vessels were washed with soap and water, soaked in 10% hydrochloric acid, then rinsed with copious Milli-Q (18.2 MΩ) water. Efforts were made to minimize pyrite oxidation and associated acid generation by excluding oxygen during leaching. Oxygen was purged from Milli-Q water by delivering ultra-high-purity N_2 gas into water through a sintered glass bubbler for 1 hour inside a glove bag. The glove bag was then filled and

purged three times with the same N_2 gas. Within the glove bag, shale in each vessel was rinsed three times with ∼5 mL of N_2-purged water. The vessels were then filled with N_2-purged water and sealed. Vessels were transferred to a stainless-steel chamber continuously purged with a flow of N_2 gas and contained within an oven set to 95 °C. Leachates were reacted for 8 days, a common duration used in leaching experiments and a factor discussed in the results section.[23,25,26,33,45] Leachate water was decanted, filtered to <0.45 μm, and splits were made for analysis of pH and dissolved constituents.

Hydrochloric acid leaches were conducted in duplicate on 2.5 g of crushed shale in acid-washed, PTFE centrifuge tubes. Each tube contained 40 mL of 0.5 M HCl. After any effervescence subsided, the tubes were sealed and shaken on a wrist shaker for 1 hour, then vented and centrifuged at 4000 rpm for 10 minutes (1.5 h total). Short reaction time limited the differential increase of pH *via* buffering by shales with different carbonate contents. Leachates were filtered to <0.45 μm. One split was analyzed for pH and another acidified with HNO_3 for analysis of dissolved elements.

Brine leaches were conducted in the same manner as water leaches, but substituting an artificial brine made using NaCl, $CaCl_2$, and $MgCl_2$ salts to yield concentrations of 41 000 mg L^{-1} Cl, 19 700 mg L^{-1} Na, 2350 mg L^{-1} Mg, and 870 mg L^{-1} Ca. These concentrations, the TDS (∼64 000 mg L^{-1}) and the ionic strength (1.4) were designed to be similar to median concentrations for well types from the PWGD. The pH of the brine leaches was measured using a calibration method for high salinity samples.[46]

Analyses of water and HCl leaches for element concentrations were conducted at USGS research laboratories in Denver, Colorado using inductively coupled plasma-mass spectrometry (ICP-MS) whereas brine leachates were analyzed with inductively couple plasma-optical emission spectroscopy (ICP-OES) and ion chromatography at the USGS Brine Research Instrumental and Experimental (BRInE) laboratory in Reston, Virginia. Complete details on leachate analyses including quality control can be found in the ESI.† All data generated for the shales and leachate experiments are publicly available online.[37]

2.4 Statistics and compositional data analysis

All statistical analyses were conducted using R (v. 3.6.0).[47] Summary statistics (median, first and third quartile) were determined by basin as identified in the PWGD for 35 elements for each of the produced waters well types. Multiple regression between parameters in the PWGD was carried out using the 'lm' function. Correlations between water characteristics (*e.g.*, pH, TDS) and concentrations of 26 elements measured in the leachate experiments were considered using the 'rcorr' function in the R package 'Hmisc'. Principal component analysis (PCA) of transformed data using the "prcomp" function in R was used to elucidate geochemical patterns in leachates and produced waters. Prior to PCA, a centered log ratio (CLR) transformation was used to place data in a compositional data analysis context. Such CLR transformation and PCA allow straightforward interpretation of relations between elements and different

1200 | *Environ. Sci.: Processes Impacts*, 2021, **23**, 1198–1219

This journal is © The Royal Society of Chemistry 2021

subsets of data permit focus on particular geochemical patterns.[48,49]

3. Results and discussion

3.1 Produced waters compositions in the United States

Data in the PWGD have great potential to yield insights into produced water chemistry but the 'as available' addition of data has resulted in an unequal representation of basin and water-type, along with a sparsity of analyte data relative to the number of samples, that pose challenges to its presentation and interpretation. Some basins and formations within basins are represented by dozens of samples, and others have only one or a few. Some samples have data for numerous trace elements, but for which elements differ between samples both within and between basins and formations. Approximately three-quarters of samples only have data for some combination of pH, TDS, Na, Ca, Mg, Cl, and SO_4^{2-}. Many more samples add only K, Fe, or Ba to that list. Such data limitations constrain the ability to make many of the analyses and comparisons that would be desired from such a theoretically broad produced waters dataset.

Two example comparisons illustrate this point. First was a comparison between conventional and unconventional produced waters from the same formations. The PWGD only contained data from multiple well types for the Bakken formation, Wolfcamp shale,[50] and Niobrara formation necessary for such an analysis, and the unconventional category only represented tight oil wells (Fig. 1). In all three cases, the number of samples was heavily skewed toward one well type, and number of samples with data decreased substantially between the major and trace elements. Nevertheless, similarity in relative elemental concentrations between conventional and tight oil produced waters composition from the same formation was observed (Fig. 1 and Table S1†). Differences in absolute major element concentrations reflected greater median salinity of the tight oil produced waters (255 000 mg L^{-1}, $n = 439$) compared to the conventional produced waters (107 000 mg L^{-1}, $n = 20$) from the Bakken formation, as well as the tight oil produced waters (44 000 mg L^{-1}, $n = 96$) compared to the conventional produced waters (15 000 mg L^{-1}, $n = 26$) from the Niobrara formation. In contrast, median salinity was only slightly greater for the tight oil produced waters (116 000 mg L^{-1}, $n = 14$) compared to the conventional produced waters
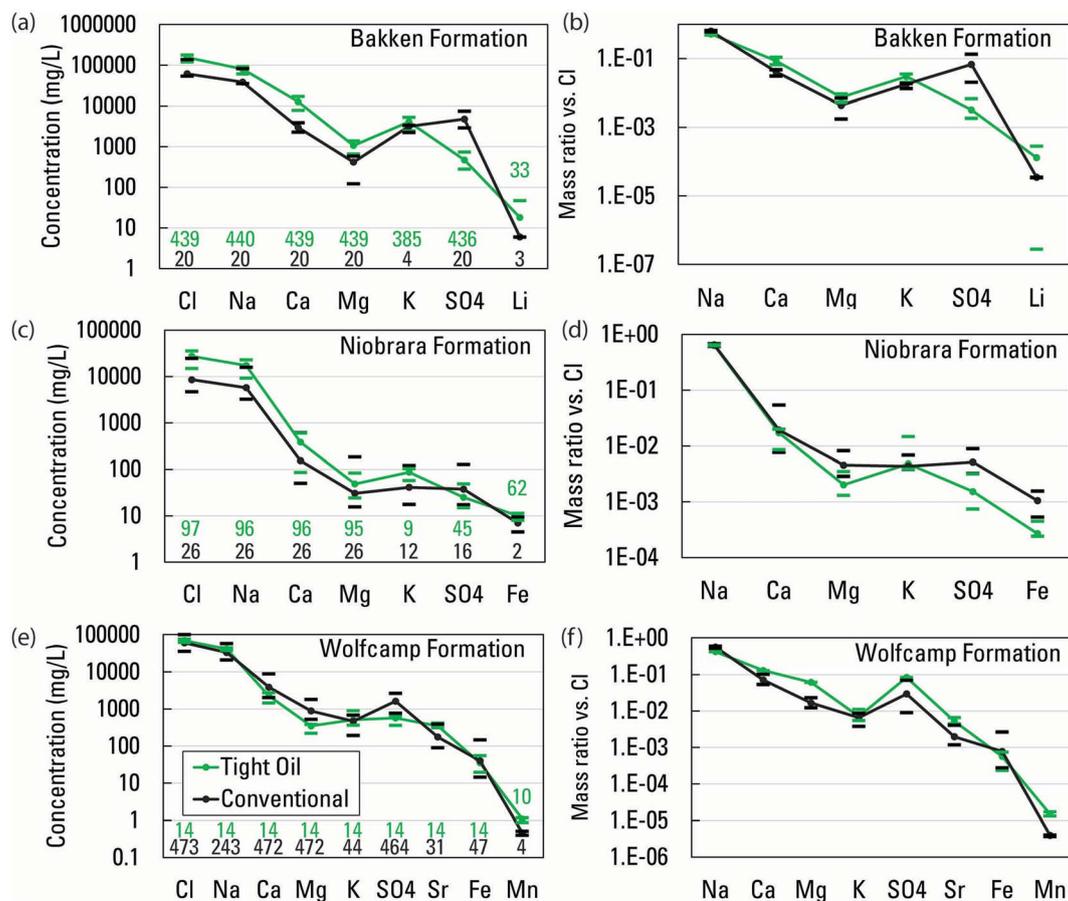

Fig. 1 Paired graphs depicting concentrations of elements in conventional and tight oil waters produced from the same formations, and mass ratios of elements to Cl. Paired graphs depict data from the Bakken formation ((a) and (b)), Niobrara formation ((c) and (d)), and Wolfcamp shale[50] ((e) and (f)) formations. All data from the USGS Produced Waters Geochemical Database (v2.3).[34] Values plotted are medians bracketed by the first and third quartiles. Number of samples per constituent per well type is indicated on each plot in (a), (c), and (e).

This journal is © The Royal Society of Chemistry 2021

Environ. Sci.: Processes Impacts, 2021, 23, 1198–1219 | 1201

(102 000 mg L^{-1}, $n = 473$) from the Wolfcamp shale. Despite the concentration differences, ratios of Na, Ca, K, and to a lesser extent Mg, to Cl indicated a common brine source for the different well types. Enhanced salinity of the unconventional waters may arise from brine or salt newly mobilized by the fracture network generated by hydraulic fracturing. Lower salinity in the conventional waters may arise from mixing with lower salinity waters made possible by the greater natural permeability in such settings. Constituents that showed some differences in ratios to Cl between well types included SO$_4$ and Mn, which could be influenced by differing redox conditions. Greater Li/Cl and Sr/Cl ratios in tight oil waters compared to conventional waters are part of a pattern discussed in Section 3.6.

A second example of the type of desirable analysis that was limited by data availability in the PWGD is trace element abundance between produced waters types and host formations. Only three formations had trace element data sufficient for a broad comparison: shale gas waters from the Marcellus shale, tight oil waters from the Bakken formation, and conventional waters from the Green River formation (Fig. 2 and Table S2†). Again, the number of samples with data decreased substantially when trace elements are considered. Lower concentrations of the major elements were present for the lacustrine Green River formation compared to the two marine formations. Distinct differences in trace element concentrations between the three formations were observed. These included notably greater Ba, Mn, and Co for the Marcellus shale and notably greater concentrations of Rb and Zn for the Bakken formation and (Fig. 2). It is likely that distinctive trace element fingerprints exist for many formations and basins, but currently the PWGD cannot offer much insight beyond these three formations.

Although detailed comparisons like those above are challenging, the PWGD provides an excellent basis for a broad understanding of produced waters chemistry. The unevenness of data availability was overcome by calculating median values of major and trace elements by source basin as identified in the PWGD (Tables S3–S8†). Medians for well types calculated from

Table 1 Median values of major and trace elements for produced waters well types calculated from basin medians. Values of pH are in standard units and concentrations of constituents are in mg L^{-1}. The number of basins per constituent is given as n. All data are from the USGS National Produced Waters Geochemical Database (v2.3).[34] See Tables S3–S8 for individual basin medians and sample counts

| Constituent	Conventional		Shale gas		Tight oil	
	Median	n	Median	n	Median	n
pH	7.3	60	6.8	5	7.2	8
TDS	30 153	61	67 458	5	78 039	9
Al	3	18	0.3	1	0.09	1
As	0.03	5	0.08	1	0.4	1
B	17	35	10	2	18	2
Ba	8	41	44	4	20	5
Br	121	39	403	2	578	3
Ca	1325	60	1130	5	1933	9
Cd	0.001	3	0.03	1	0.05	1
Cl	16 688	60	42 000	5	46 431	9
Co	0.004	2	0.5	1	0.03	1
Cr	0.1	3	0.03	1	0.5	1
Cs	0.2	17	0.2	2	0.004	1
Cu	1	12	0.3	1	0.04	1
F	2	11	3	1	8	1
Fe	12	46	24	5	24	7
I	10	40	15	2	48	3
K	100	56	263	5	315	7
Li	5	45	12	3	18	1
Mg	175	60	834	5	264	9
Mn	2	22	2	2	0.6	2
Mo	0.004	1	0.05	1	0.01	1
Na	8267	59	19 700	5	24 715	9
Ni	0.07	3	0.1	1		0
P	0.7	10	0.07	1		0
Pb	0.03	7	0.03	1	0.03	1
Rb	0.6	19	0.8	1	14	1
S	43	12	3	1		0
SO$_4$	414	60	50	5	67	9
Sb	0.001	1	0.1	1		0
Se	0.2	6	0.05	1	1	1
Si	28	34	6	1	14	1
Sr	84	45	951	2	559	2
Ti		0	0.2	1		0
Tl		0	0.1	1		0
U	0.009	1		0	0.003	1
V	0.4	1		0	0.9	1
Zn	2	14	0.2	1	13	1
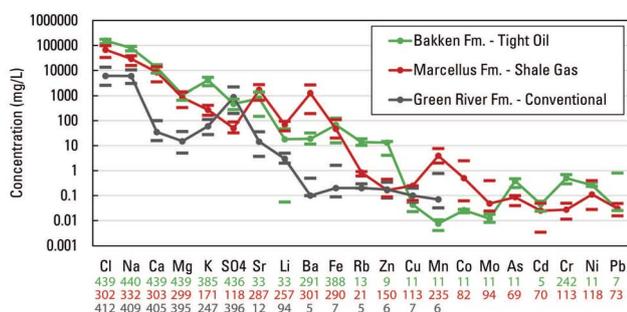
Fig. 2 Concentrations of elements in produced waters for three formations that have relatively great abundance of trace element data in the USGS Produced Waters Geochemical Database (v2.3):[34] the Bakken, Marcellus, and Green River formations. Values plotted are medians bracketed by the first and third quartiles. Number of samples per constituent is indicated below the plot. Fm., formation.

those basin medians provided broad characterization of produced waters chemistry (Table 1). For example, the median total dissolved solids (TDS) for waters from conventional wells was about 30 000 mg L^{-1} (range of medians 6200–285 900 mg L^{-1}, $n = 61$ basins) (Fig. S1†). By comparison, waters from shale gas wells were more saline with median TDS of about 67 000 mg L^{-1} (15 700–112 600 mg L^{-1}, $n = 5$), as were waters from tight oil wells with median TDS of about 78 000 mg L^{-1} (16 800–254 500 mg L^{-1}, $n = 9$). The pH of produced waters can be similarly summarized. Conventional produced waters had a median pH of 7.3 (5.7–8.2, $n = 60$), those from shale gas wells had a median pH of 6.8 (6.5–7.7, $n = 5$), and those from tight oil wells had a median pH of 7.2 (6.0–7.7, $n = 8$) (Fig. S1†). Such summaries indicate that unconventional waters generally have

1202 | *Environ. Sci.: Processes Impacts*, 2021, **23**, 1198–1219

This journal is © The Royal Society of Chemistry 2021

greater salinity than conventional waters but belies the facts that ranges overlap substantially, and many conventional waters are quite saline (Fig. S1†). Additionally, the lower median pH of shale gas waters might reflect some contributions of

flowback of acidified hydraulic fracturing water rather than formation conditions.

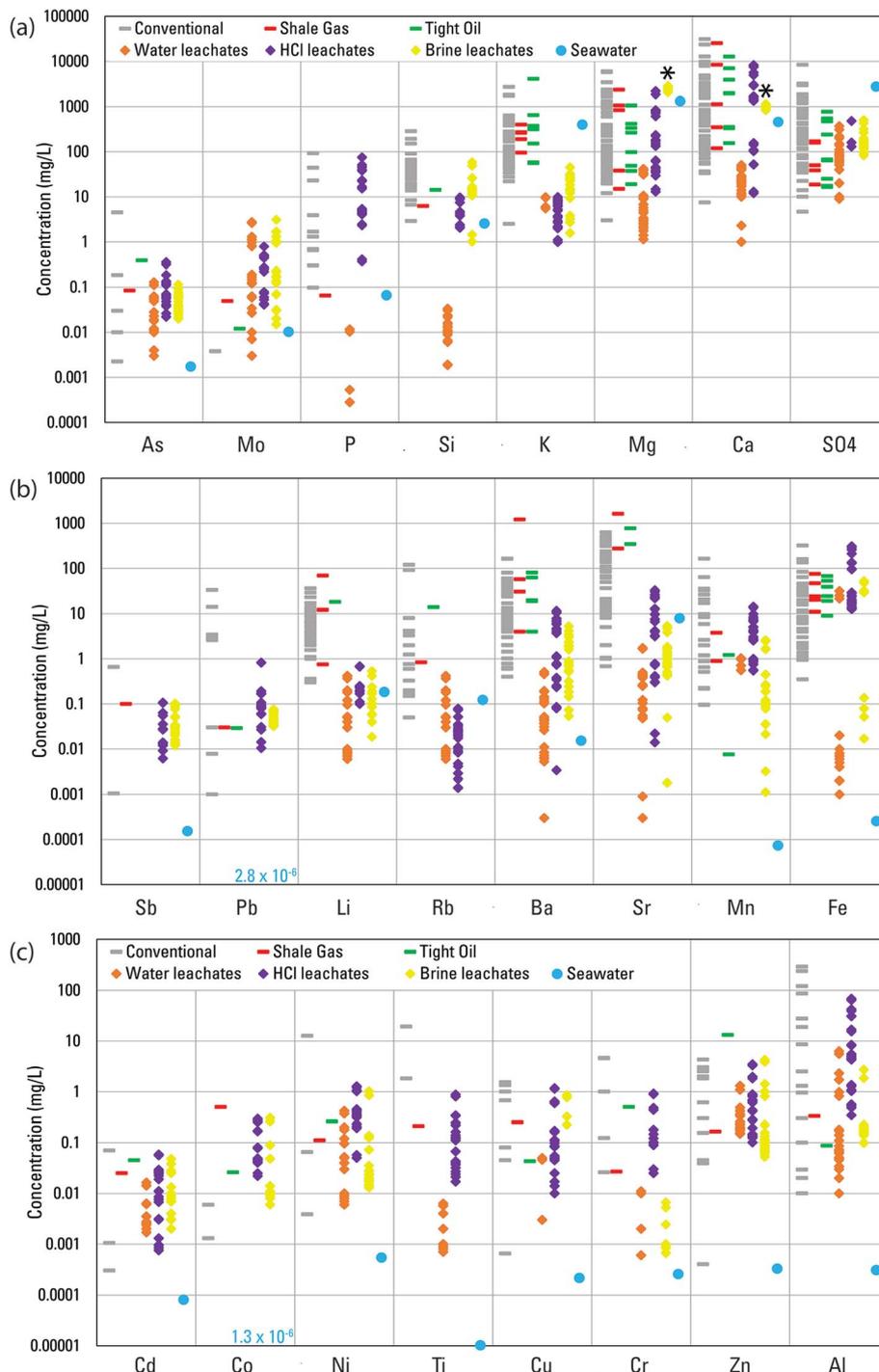The number of basins that have data to assess concentrations of major and trace elements varied substantially. Those numbers, and medians of basin medians are summarized in

Fig. 3 Median concentrations in individual basins for (a) As, Mo, P, Si, K, Mg, Ca, SO₄²⁻, (b) Sb, Pb, Li, Rb, Ba, Sr, Mn, Fe, and (c) Cd, Co, Ni, Ti, Cu, Cr, Zn, Al in produced waters from different well types in the USGS Produced Waters Geochemical Database (v2.3).[34] Also plotted are concentrations in the water, HCl, and artificial brine leachates. Concentrations in modern seawater are provided for reference.[51] Asterisks indicate constituents (Ca and Mg) used to create the artificial brine prior to reaction with shale. Seawater concentrations less than the lower limit of the y-axis are printed on the figure.

This journal is © The Royal Society of Chemistry 2021

Environ. Sci.: Processes Impacts, 2021, **23**, 1198–1219 | **1203**

Table 1. Medians of major and trace elements for individual basins and the number of samples upon which those medians are based are summarized in Tables S3–S8.† In Fig. 3, the individual basin medians are plotted for 24 elements. The ranges of those medians indicate that typical concentrations of most elements among different produced waters range over three orders of magnitude. Chromium, Li, and Si are notable in ranging over only two orders of magnitude and Al, Ba, and Pb are notable in ranging over four orders of magnitude. Controls

on element concentrations and their wide-ranging variability are the focus of the remainder of the paper.

Concentrations of elements in produced waters broadly reflect the following: (1) inheritance from paleo-seawater, seawater-derived evaporites, and bitterns and (2) water–rock interactions with the minerals and organic matter present in conventional oil and gas reservoir rocks or shale reservoirs.[14,16] Therefore, comparisons to concentrations in modern seawater provided a point of reference for understanding concentrations
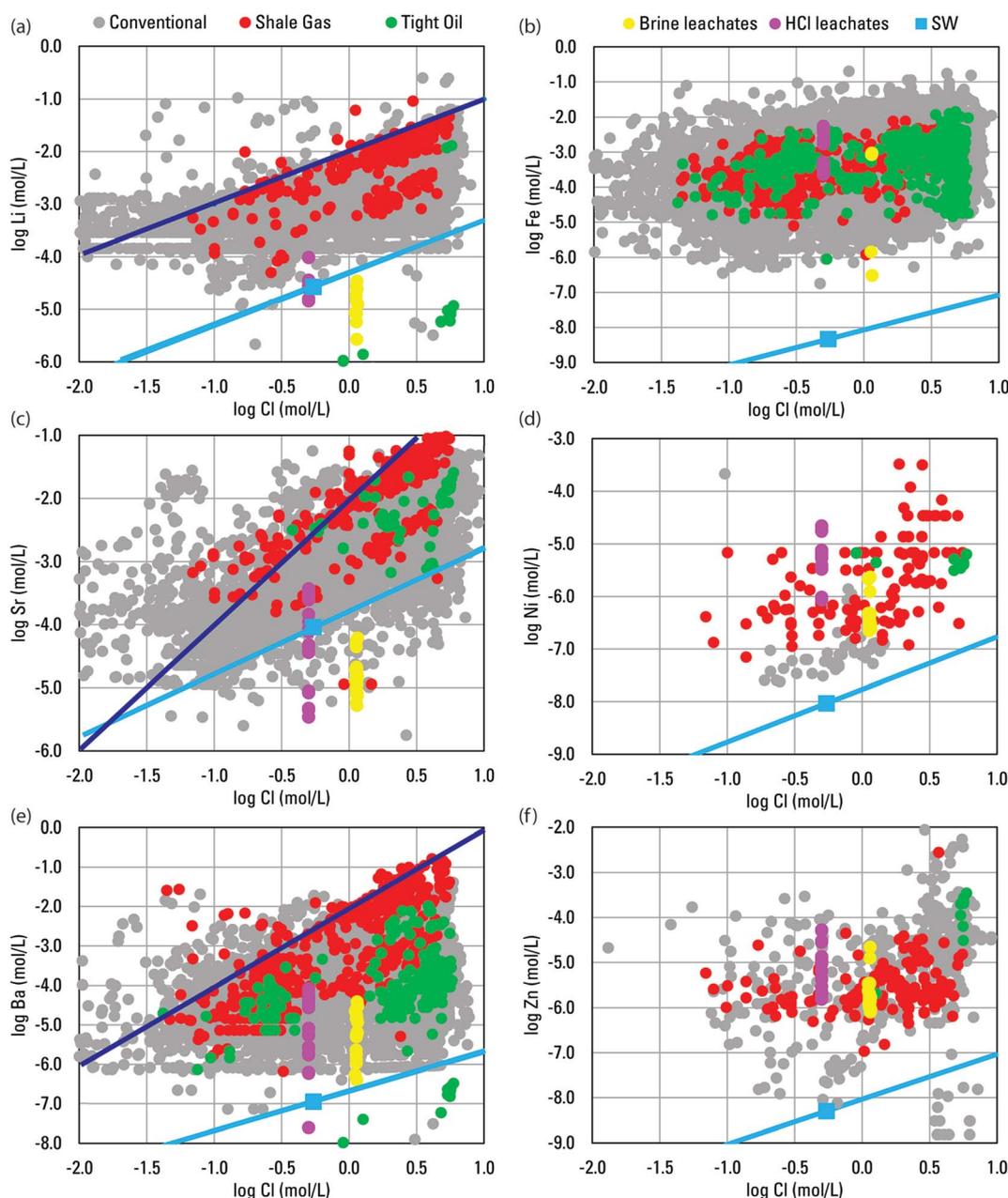

Fig. 4 Scatterplots comparing log molar concentrations of Cl in produced waters well types and brine and HCl leachates to log molar concentrations of Li (a), Fe (b), Sr (c), Ni (d), Ba (e), and Zn (f) for individual samples from the USGS Produced Waters Geochemical Database (v2.3).[34] For reference, concentrations in seawater are plotted along with a light blue line indicating an evaporation/dilution trend for seawater that does not account for halite or other mineral saturation. Also, for reference, darker blue lines indicate an arbitrary 1 : 1 slope in (a) and arbitrary 2 : 1 slope in (c) and (e).

1204 | Environ. Sci.: Processes Impacts, 2021, 23, 1198–1219

This journal is © The Royal Society of Chemistry 2021

of certain elements (Fig. 3).[51] The most generally abundant elements in produced waters, Na and Cl (Tables 1 and S3–S8†), had basin median concentrations in produced waters that ranged about one order of magnitude greater than and less than seawater for Na and somewhat more widely for Cl (Fig. S2†). That variation reflected derivation from paleo-seawater, evaporative concentration, mixing with meteoric waters, evaporite dissolution, and/or halite solubility.[14] Roughly half of basin-median Na and Cl concentrations were greater than modern seawater, the case being more common for unconventional waters (Fig. S2†). Sulfate, Mg, and K, by contrast, all tended to have basin-median concentrations similar to or lower than to seawater (Fig. 3a), reflecting redox influence on SO_4^{2-} and dissolution/precipitation reactions with sulfate and sulfide minerals; loss of Mg from solution by formation of dolomite, ankerite, and chlorite; and loss of K from solution by the illitization of smectite.[14] For essentially all other elements, basin-median concentrations in most produced waters were greater than in seawater, in many cases by several orders of magnitude (Fig. 3).

With the exception of Na and Cl, concentrations of dissolved elements in produced waters are considered to be strongly influenced by water–rock interaction, also termed

thermodynamic buffering or rock-buffering.[52,53] For the major elements, interactions with silicate-carbonate mineral assemblages tend to generate 1 : 1 slopes on log molar plots with Cl for K, which occurs as a monovalent cation, and 2 : 1 slopes for Mg and Ca which occur as divalent cations.[17,53] Such patterns were generally observed for individual samples in the PWGD, although they were more apparent for the shale gas and tight oil samples (Fig. S3†). For the trace elements, the same general 1 : 1 slope was observed for monovalent Li, a general 2 : 1 slope was observed for divalent Ba, and a slope somewhat less than 2 : 1 was observed for divalent Sr (Fig. 4). Such patterns indicated that similar water–rock interactions generally control the trace alkali and alkali earth elements as the major elements. For other trace elements, like Fe, Ni, and Zn, general positive trends with Cl were apparent but identifiable molar slopes were not (Fig. 4).

The observed slopes and positive trends indicate enhanced mobilization with increased Cl, the dominant source of anionic charge in highly saline produced waters.[17] Chloride has been described as the master variable in controlling produced water chemistry and it enhances element solubility by complexing with cations in solution and decreasing solution pH.[52,54] Increases in Cl concentration drive increases in the activity of
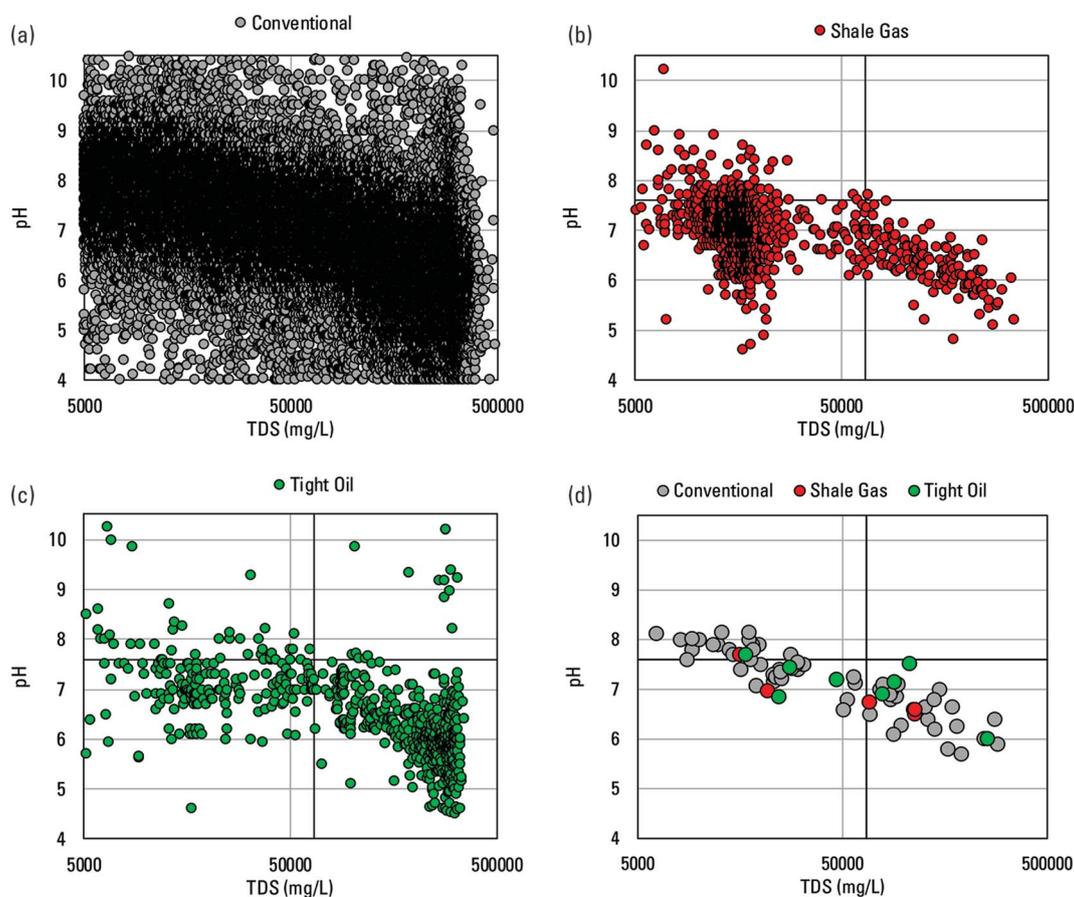

Fig. 5 Scatterplots of TDS *versus* pH (standard units) for conventional (a), shale gas (b), and tight oil (c) samples of produced waters, and basin median values for all three types (d) from the USGS Produced Waters Geochemical Database (v2.3).[34] For reference, the median TDS and pH values of the brine leachates are plotted as black vertical lines, respectively, in (b), (c) and (d). A curve towards lower pH values at the highest TDS values is visible in (a) and (c) and a more linear relation is visible in (b) and (d).

This journal is © The Royal Society of Chemistry 2021

Environ. Sci.: Processes Impacts, 2021, **23**, 1198–1219 | **1205**

H^+ and a pronounced decrease in pH to more commonly include values between 4 and 6 when TDS is >100 000 mg L^{-1} has been shown for sedimentary basins worldwide.[17] Conventional and tight oil produced waters samples in the PWGD showed a similar pattern (Fig. 5a and c). Additionally, conventional and shale gas produced waters samples and basin medians showed a general relation between increasing TDS and decreasing pH that spanned a broader range of TDS (Fig. 5 a, b and d).

A second substantial driver of pH in produced waters can be dissolved CO_2. Discerning the relations between CO_2 and pH in produced waters, or between pH and trace elements, can be a challenge because degassing of CO_2 and other acid volatiles can change their concentrations and raise pH by 1–2 units before measurement at the surface.[14] In the PWGD, testing both parameters together in multiple regression, the pH of shale gas waters was significantly correlated ($p \leq 0.05$) with TDS ($p < 0.001$) and CO_2 ($p < 0.001$) across 925 samples. However, the pH of conventional waters was significantly correlated with TDS ($p < 0.001$) but not CO_2 ($p = 0.95$) across 137 samples and pH of tight oil waters was not significantly correlated with TDS ($p = 0.44$) or CO_2 (0.40) across 85 samples. Smaller pools of data may have obscured the relations in the latter two categories.
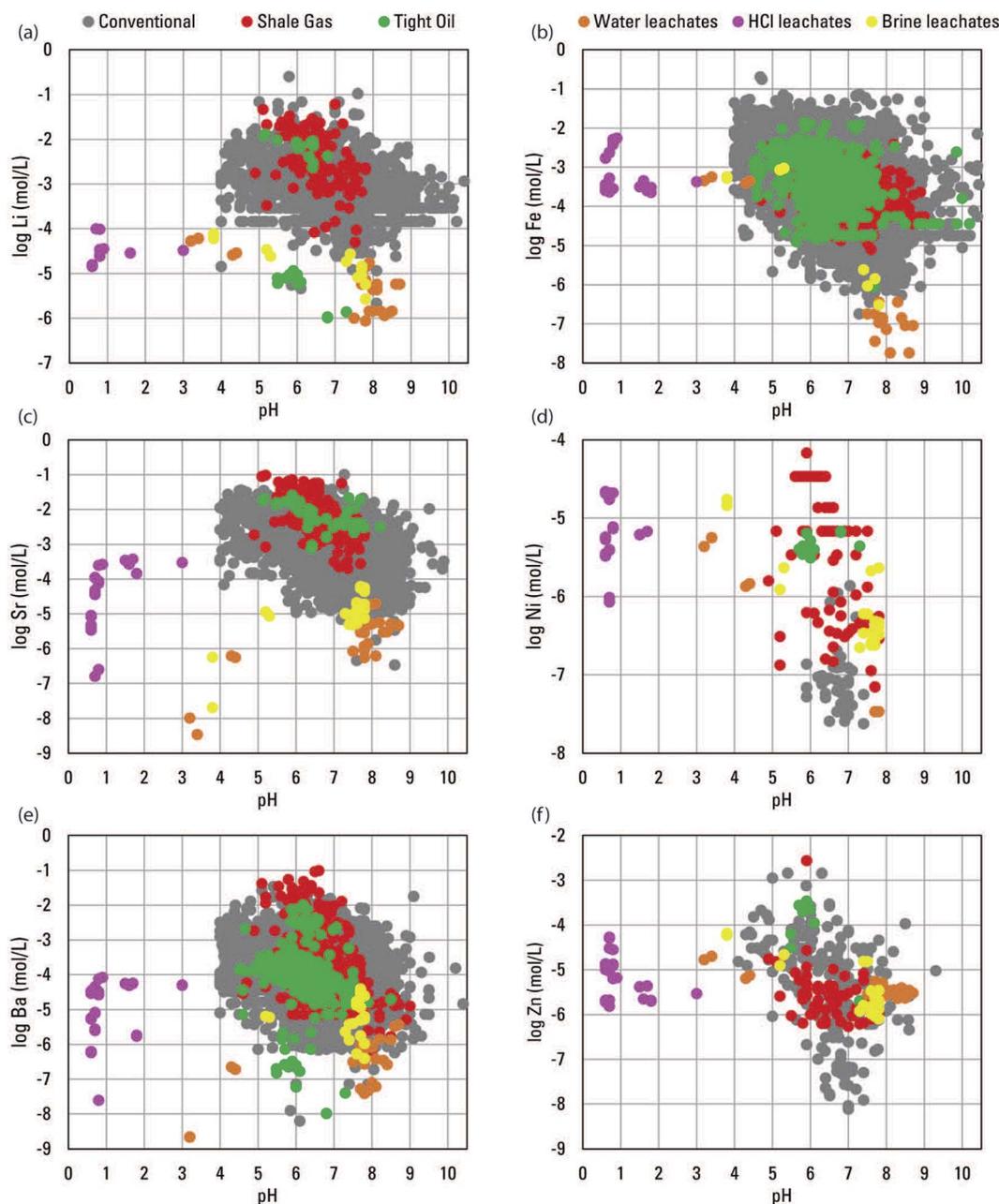

Fig. 6 Scatterplots comparing the pH of produced waters well types from the USGS Produced Waters Geochemical Database (v2.3)[34] and water, HCl, and brine leachates to log molar concentrations of Li (a), Fe (b), Sr (c), Ni (d), Ba (e), and Zn (f).

1206 | Environ. Sci.: Processes Impacts, 2021, 23, 1198–1219

This journal is © The Royal Society of Chemistry 2021

Because CO_2 is a second influence on pH, it is possible that some of the variability in element concentrations in produced waters can be correlated to pH independently of Cl. However, in contrast to relations with Cl (Fig. 4 and S3†), relations between elements and pH were apparent but less distinct (Fig. 6 and S4†). Multiple regression was used to assess whether pH and Cl were significant influences on trace element concentrations in conventional produced waters, and whether their influences were distinct. A similar analysis was not conducted for unconventional waters because of the chance that dilution by flow-back water in some samples might artificially correlate Cl with other elements. In conventional waters, many elements were significantly positively correlated with Cl, and some were also significantly negatively correlated with pH (Table 2). The variance in pH driven by CO_2 in produced waters may be less influential than that from ionic strength and thereby mute the independent influence of pH. Generally, elements with more available data more commonly had significant correlations, indicating more correlations might be found with additional data (Table 2). Elements like Na and K that were predominantly sourced from seawater (Fig. 3) likely correlate with Cl because of that sourcing, and with pH due to autocorrelation. However, for elements predominantly sourced from water–rock interaction, the results and interpretations are less clear. For some, like Al

Table 2 P-values and number of samples for multiple regression analysis of pH and Cl correlation with dissolved element concentrations in conventional produced waters from the USGS National Produced Waters Geochemical Database (v2.3).[34] Values < 0.05 are shown in bold

Element	pH	Cl	n
Al	**0.005**	**0.01**	164
As	**0.02**	**<0.0001**	48
B	0.31	**<0.0001**	1450
Ba	0.07	**<0.0001**	6336
Br	**0.01**	**<0.0001**	2081
Ca	**<0.0001**	**<0.0001**	57 622
Cd	0.42	**<0.0001**	52
Co	0.12	0.41	40
Cr	**0.01**	0.56	1375
Cs	0.91	0.07	261
Cu	0.34	0.57	234
F	0.65	0.36	286
Fe	**<0.0001**	**<0.0001**	13 669
K	**<0.0001**	**<0.0001**	14 340
Li	**<0.0001**	**<0.0001**	3588
Mg	**<0.0001**	**<0.0001**	56 955
Mn	0.35	**<0.0001**	724
Mo	0.35	0.63	11
Na	**<0.0001**	**<0.0001**	53 727
Ni	0.45	0.33	43
P	0.32	0.65	20
Pb	0.56	0.55	78
Rb	0.83	**<0.0001**	431
SO4	**<0.0001**	**<0.0001**	51 334
Se	0.58	**<0.0001**	77
Si	0.06	0.48	1685
Sr	**<0.0001**	**<0.0001**	4435
Zn	0.36	0.24	366

and As, both pH and Cl were significant and for others like Cu, Ni, and Zn, neither were significant (Table 2). Ultimately though, discerning between the combined pH and complexation effects of Cl and distinctive effects of pH in produced waters is difficult. The shale leachate experiments offer better insight in that regard.

3.2 Shale–leachate experiments

Element mobilization by water–rock interaction is controlled in part by the elemental composition and mineralogy of the rock. The 12 shales used in the experiments show overlap for major and trace elements with reference compositions, such as the North American shale composite (NASC)[55] (Fig. S5†), although the comparatively high carbonate content of the Boquillas and Niobrara formations, and the Uteland Butte member of the Green River formation (Tables 3, S9 and S10†) dilute the concentrations of many elements. Leachate results showed no patterns relative to shale organic matter thermal maturity, so shales and leachates were categorized by shale mineralogy (Tables 3, S9 and S10†). The Mancos shale and Cow Ridge member of the Green River formation formed a low-carbonate group [<0.02 wt% inorganic carbon (IC)]. The Woodford shale, Bakken formation, and the Garden Gulch and Parachute Creek Members of the Green River formation formed a high organic carbon group (>10 wt% organic C). The remaining six shales formed an intermediate group.

Chloride was below the 0.6 mg L^{-1} reporting limit in water leaches from 5 of the shales and ranged from 0.8–8 mg L^{-1} in 6 others. Water leachates from shale of the Bakken formation averaged 57 mg L^{-1} Cl but had lower Na concentrations than two other shales. Thus, contributions from brine salts trapped in shale to element concentrations in leachates were considered minimal.

The final pH values of the leachates had substantial influence on element mobilization and were a function of both leachate and shale mineralogy. The deionized water leachates had a median pH of 7.9, but acidic pH values were measured for the low-carbonate Mancos (3.3) and Cow Ridge (4.4). In contrast, the median pH of the HCl leachates was 0.8, but the three shales having the greatest wt% IC (Boquillas, Niobrara, and Uteland Butte) yielded leachates with moderately higher pH values (1.5–3.0). The brine leachates were generally circumneutral (median pH 7.6), but again the two low-carbonate shales yielded acidic pH values (Mancos, 3.8; Cow Ridge, 5.3).

Pyrite oxidation was a substantial source of acidity for the water and brine leachates, despite efforts to mitigate this effect, as indicated by median concentrations of SO_4^{2-} in both leachates of 73 mg L^{-1} (range 9–370 mg L^{-1}) and 153 mg L^{-1} (range 83–505 mg L^{-1}), respectively (Fig. 3a). For the HCl leachates, only leachates of the Cow Ridge (145 mg L^{-1}) and Mancos (480 mg L^{-1}) leachates exceeded the 100 mg L^{-1} lower reporting limit for SO_4^{2-}. Oxidation was likely enabled by incomplete exclusion of oxygen from the water and brine experiments by the N_2 purge gas. Pyrite oxidation is a common theme in shale leaching experiments, as is the variable presence of carbonates to buffer the resulting acidity.[25–27,30–33,56] X-ray diffraction (XRD)

This journal is © The Royal Society of Chemistry 2021

Environ. Sci.: Processes Impacts, 2021, **23**, 1198–1219 | **1207**

Table 3 Selected properties of the shales used in the leachate experiments. Concentrations of organic and inorganic C and total S. Quantitative mineralogy results for a subset of minerals, with ND indicating no detection above the threshold of 1 wt%. Shales are categorized as described in the text

Identifier	Sample description	Category	Org. C, (wt%)	Inorg. C, (wt%)	Tot. S, (wt%)	Calcite, (wt%)	Dolomite, (wt%)	Illite, (wt%)	Pyrite, (wt%)
Shale-1	Uteland Butte mem. (inf.[41–43]) of Green River Fm.	Intermediate	2.4	12	<0.05	12	87	ND	ND
Shale-2	Marcellus shale of Hamilton group	Intermediate	4	0.11	2.7	4	ND	33	4
Shale-3	Marcellus shale of Hamilton group	Intermediate	2.5	1.9	1.2	15	ND	25	2
Shale-4	Barnett formation	Intermediate	3.1	2.1	1.7	7	10	14	2
Shale-5	Bakken formation	High organic	11.8	0.4	3.6	2	4	25	5
Shale-6	Niobrara formation	Intermediate	4.4	8.6	1.5	85	ND	4	3
Shale-7	Parachute Creek member of Green River formation	High organic	14.2	4.9	0.6	10	44	ND	ND
Shale-8	Garden Gulch member of Green River formation	High organic	12.9	2.4	1.9	ND	18	26	2
Shale-9	Cow Ridge member of Green River formation	Low carbonate	8.7	0.01	0.4	ND	ND	25	ND
Shale-10	Boquillas formation	Intermediate	2.0	9.9	0.5	77	7	ND	ND
Shale-11	Mancos shale	Low carbonate	3.0	0.01	0.8	3	ND	32	ND
Shale-12	Woodford shale	High organic	12.3	2.2	3.2	ND	16	10	2

analysis quantified pyrite in seven of the shales in the 2–5 wt% range (Table 3), four others contained 0.4–0.8 wt% S, a substantial portion of which is likely in pyrite, and only shale from the Uteland Butte contained <0.05 wt% S. However, neither wt% pyrite nor S content predicted SO_4^{2-} in the water or brine leachates ($R^2 < 0.03$ and $p > 0.5$ for both). Variation of leachate SO_4^{2-} may be influenced by pyrite surface area, as kinetic control of pyrite oxidation rates has been observed in other shale-leaching experiments.[26]

Controls on the mobilization of elements can be categorized by their concentration responses to the pH and ionic strength conditions in the different leachates. In other shale-leaching studies, lower pH fluids enhanced mobilization of nearly all elements and was the primary control for some.[25–27,33,56,57] In this study, the first category of elements was generally marked by the 0.5 M HCl leach extracting their largest fractions relative to shale, and by strong negative correlations (greater acidity correlating with greater concentrations) between leachate pH and element concentration for both the water and brine (Table S11,† and Fig. 7). Such elements include most of the transition metals considered, Cd, Co, Cr, Cu, Fe, Mn, Ni, Ti, and Zn, but also Al, Mg, P, and Rb. Similar acidity influence was apparent for the second category, but for Si, As, Pb, and Li, ionic strength was a second notable influence on mobilization. For Si, slightly greater concentrations were measured in the brine *versus* HCl leachate (Fig. 7). For As and Pb, the HCl leachate extracted the largest fraction, but correlations with pH indicating enhanced mobility were absent in the water and brine extracts (Table S11†). For Li, slightly greater fractions were extracted by the brine and pH was a strong influence (Table S11†). Mobilization of elements in the third category appeared to be less influenced by pH and more by ionic strength, based upon the highest concentrations being achieved by the brine and lack of strong correlations with pH. As observed in another study, this was the

case for K, Mo, and Sb (Table S11†).[27] The large fraction of Mo extracted by the water leachate indicates a general lability,[57] an effect attributed elsewhere to Mo release from organic matter by diagenesis.[58] A final category includes elements substantially influenced by acidity but associated with carbonates that provide buffering capacity, as interpreted by positive correlations with pH (Table S11†). These include the alkali earth metals Ca, Sr, and Ba. The categorizations are relative to the current experiments, and other shale leaching experiments that tested increasing ionic strength from 0.03 to 0.9 showed markedly enhanced mobilization of K, Sr, Rb, and Ba and positive but lesser influence on Ca, Mg, Mn, SO_4^{2-}, Al, As, Cu, Li, P, Pb, Sb, Ti, V, and Zn.[31]

Shale mineralogy and organic matter also influenced element mobilization. Both As and Mo had greater leachate concentrations in the high-organic-carbon shales, a pattern observed in other experiments.[26,27] Hints of this pattern existed for other elements (Fig. 7), and many elements, like Cr, Cu, and Ni, associate with organic carbon in shale.[16] The organic fraction in shales can contain approximately double the trace element content of the carbonate or sulfide fractions.[15] The greatest concentrations of the primarily pH-affected elements in the leachate generally correlated with the poorly buffered, low-carbonate shales (Fig. 7). The carbonate-associated elements (*i.e.*, Ca, Sr, and Ba) generally had lower concentrations in the low-carbonate shale leaches. Studies of the Marcellus shale have indicated that Ba and to a lesser extent Sr may be mobilized largely from exchange sites.[33,45,59] Results here indicated that when more carbonate is present, carbonate is the major source of Ba to associated fluids. Barium concentrations in leachates positively correlated with shale carbonate content for the water ($R^2 = 0.53$, $p < 0.001$) and HCl ($R^2 = 0.19$, $p = 0.03$) leachates, as did Sr concentrations in HCl ($R^2 = 0.71$, $p < 0.001$) and brine ($R^2 = 0.24$, $p = 0.02$) leachates. Additionally, all the
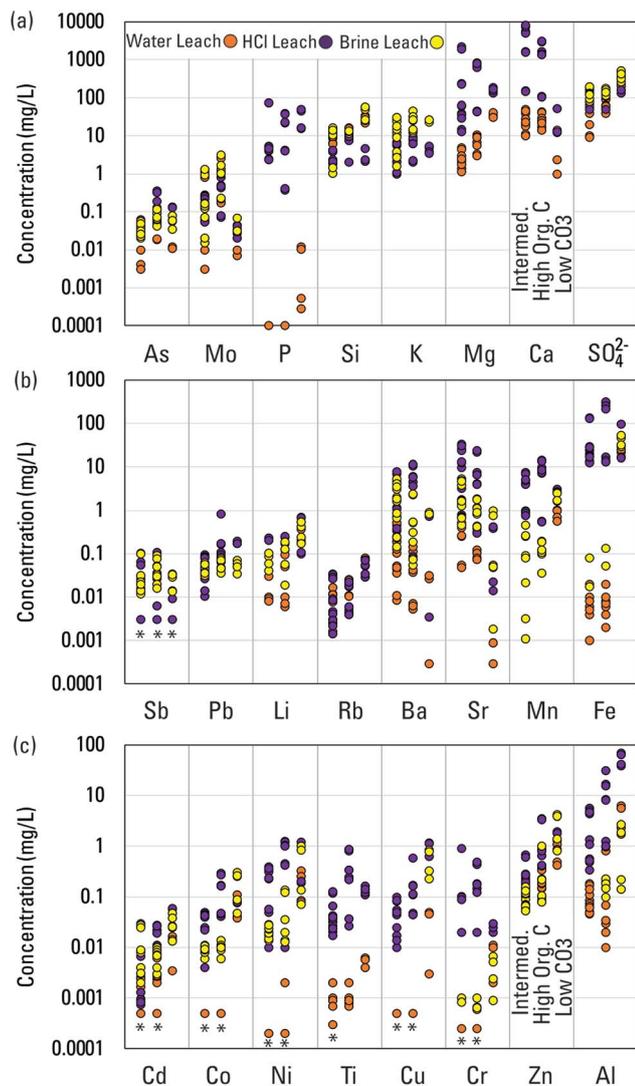
1208 | *Environ. Sci.: Processes Impacts*, 2021, **23**, 1198–1219

This journal is © The Royal Society of Chemistry 2021

Fig. 7 Concentrations of elements in the three leachate types (deionized water, 0.5 M HCl, artificial Na, Ca, Mg−Cl brine with ionic strength of 1.4). Order of elements in (a)−(c) is the same as in Fig. 1. Asterisks indicate values of half the detection limit plotted for certain samples for reference. Samples are plotted by shale mineralogical categories discussed in the text with the order shown on the figure.

leachates generally extracted >10× more Ba and Sr from the other shales compared to the low-carbonate shales (Fig. 7) despite moderate concentrations of Ba and Sr in the low-carbonate shales.[37] One factor possibly limiting Ba concentrations in leachates was barite precipitation. Barite saturation indices were calculated for the leachates using the PHREEQC program and the PHREEQC (water, HCl) Pitzer (brine) databases.[60] Only leachate water from the Niobrara formation was saturated relative to barite, though some others were in the −0.1 to −0.3 range. The brine leachates from both samples from the Marcellus shale and shale samples from the Niobrara formation, and the Cow Ridge and Parachute Creek members of the Green River formation were saturated to oversaturated relative to barite. No leachates were saturated relative to gypsum or celestite.

A more holistic view of element associations and controls on element mobilization was possible through the application of PCA to CLR-transformed shale leachate composition data (Fig. 8). The combinations of elements for which data above reporting limits were available varied from one leachate type to another, but patterns were nevertheless apparent. In each biplot (Fig. 8), a relation driven by pH can be imagined by drawing a line from the samples with the greatest carbonate buffering capacity (shales 1, 6, 7, and 10) to the low-carbonate samples (shales 9 and 11). Compositions from the carbonate-buffering end of the spectrum were more dominated by alkaline earth elements Ca, Sr, and Ba, and in the HCl leachates, also Mg. Such elements were predominantly sourced from carbonate dissolution. The poorly buffered samples had compositions more generally dominated by the transition elements and other trace elements that were more effectively mobilized under low pH conditions. A few elements had influence orthogonal to the pH trend. In the water leachates, Mo and As, the potentially more organic-associated elements were notable. In the brine leachates, K and Mn were notable, and possibly As, Pb, and Sb. Reasons for these patterns were unclear. Nevertheless, the dominant pattern in all three leachate types was a distinction between compositions emphasizing alkaline earth elements *versus* transition and other trace elements.

3.3. Shale–leachate interactions and rare earth elements

Rare earth element (REE) data were available for the water and HCl leachates, and their relations to overall leachate composition using PCA were represented by the light REE (LREE) (using Nd) and by the middle REE (MREE) (using Gd) (Fig. 8a and b). In the water leachates, Nd and Gd oriented toward the lower pH leachates, indicating more mobilization under lower pH conditions. In the HCl leachates, Nd and Gd were slightly out of line with the pH trend, and they associated with the K trend indicating a possible link to illite.

The bulk shales had REE concentrations that showed slight MREE enrichment compared to the NASC in some cases (Fig. 9a). Such slight enrichments relative to shale reference compositions have been noted elsewhere.[61,62] Concentrations of REEs in the water leachates were low, and most showed little relative enrichment compared to bulk shale (Fig. 9b). However, the lower pH water leachates of shales 9 and 11 showed patterns like those in the HCl leachates. Almost all the HCl leachates showed MREE enrichment compared to bulk shales (Fig. 9c). The leachate patterns are informative because REE concentrations in produced waters have received little study[38] and no REE data exist in the PWDB. Sharp, positive Eu anomalies have been measured in produced waters, sometimes with minor Sm and Gd riders, but not the broad MREE enrichment seen in the leachates.[38] Acidic weathering of sedimentary materials tends to generate MREE enrichment without a sharp Eu anomaly in the resulting fluids, a pattern usually attributed to dissolution of a MREE-enriched phosphate phase.[63,64] Here, mobilization of REEs did not correlate significantly with mobilization of P in the HCl leachates, but mobilization of the MREEs did correlate with the illite-associated elements K and Rb (Fig. S6†). Additionally,

This journal is © The Royal Society of Chemistry 2021

Environ. Sci.: Processes Impacts, 2021, **23**, 1198–1219 | **1209**
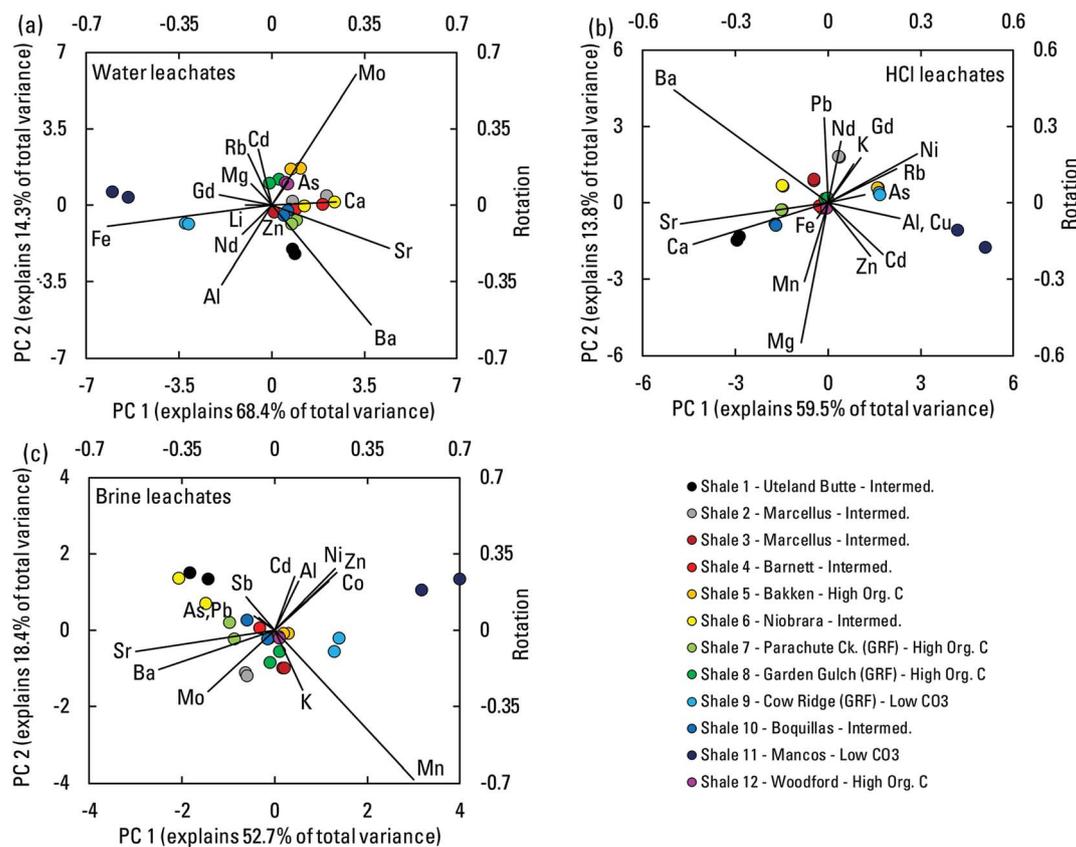
Fig. 8 Biplots of results from principal component analysis of centered log ratio transformed compositions of the water (a), HCl (b), and artificial brine (c) leachates. Sample scores for principal components (PC) 1 and 2 are plotted on the primary axes. Rotations for the included elements are plotted as rays on the secondary axes. Combinations of elements differ among the analyses depending upon detection above reporting limits in the different leachates. Cow Ridge, Uteland Butte (informal[41–43]), Garden Gulch, and Parachute Creek are members of the Green River formation. Mem., member.

concentrations of MREE in the HCl leachates correlate positively with illite abundance in shale, but LREE do not (Fig. S7†). The results indicate that MREE enrichment in produced waters relative to host shale can result from lower pH water–rock interaction, but that the sharp Eu anomalies observed in some produced waters arise from some process not replicated here.

3.4. Laboratory leachates compared to produced waters

Of the three leachate types, the brine leachates may be the most useful for comparison to produced waters because they approximated their ionic strength but the contrasting ionic strength and pH of the water and HCl leachates provide context for interpretations. The brine leachates achieved concentrations that generally approximate produced waters for many elements including Al, As, Cd, Co, Cu, Mo, Ni, Pb, Sb, Si, and Zn (Fig. 3). The approximations are notable for several reasons. First, they indicate that the mineral or organic sources of these elements were not depleted despite the greater water–rock ratios in the leachates compared to formation waters and that conditions approaching equilibrium may have been achieved by the leachates. Second, the approximations were notable because solubilities of many of the elements listed are particularly responsive to decreases in pH and the pH values of many

of the brine leachates are somewhat greater than many produced waters (Fig. 6 and S1†). However, many of these elements also form complexes with Cl and concentrations of Cl in the brine leachates are similar to many produced waters (Fig. 4). Concentrations of Fe, and Mn in the brine leachates in most cases were low compared to produced waters (Fig. 3). It is possible that differences in redox conditions in the leachates compared to the subsurface played a role in limiting leachate Fe and Mn mobilization. Concentrations of K, Li, Sr, Ba, and Cr in the brine leachates were quite low compared to produced waters. Potassium is easily explained as being generally inherited from seawater rather than derived from water–rock interaction. Rubidium concentrations in the HCl leachates are also low relative to produced waters and the high concentrations in many produced waters is attributed to discrimination against Rb as K and Rb are immobilized by illitization.[65] Little is known about controls on Cr in produced waters but the distinction between the HCl and brine leachates indicate that Cr is more sensitive to pH than ionic strength effects. The pattern may be attributable to the predominantly anionic forms of Cr in solutions that would not complex with Cl. The patterns regarding Li, Sr, and Ba are discussed in greater detail in Section 3.6.

1210 | *Environ. Sci.: Processes Impacts*, 2021, **23**, 1198–1219

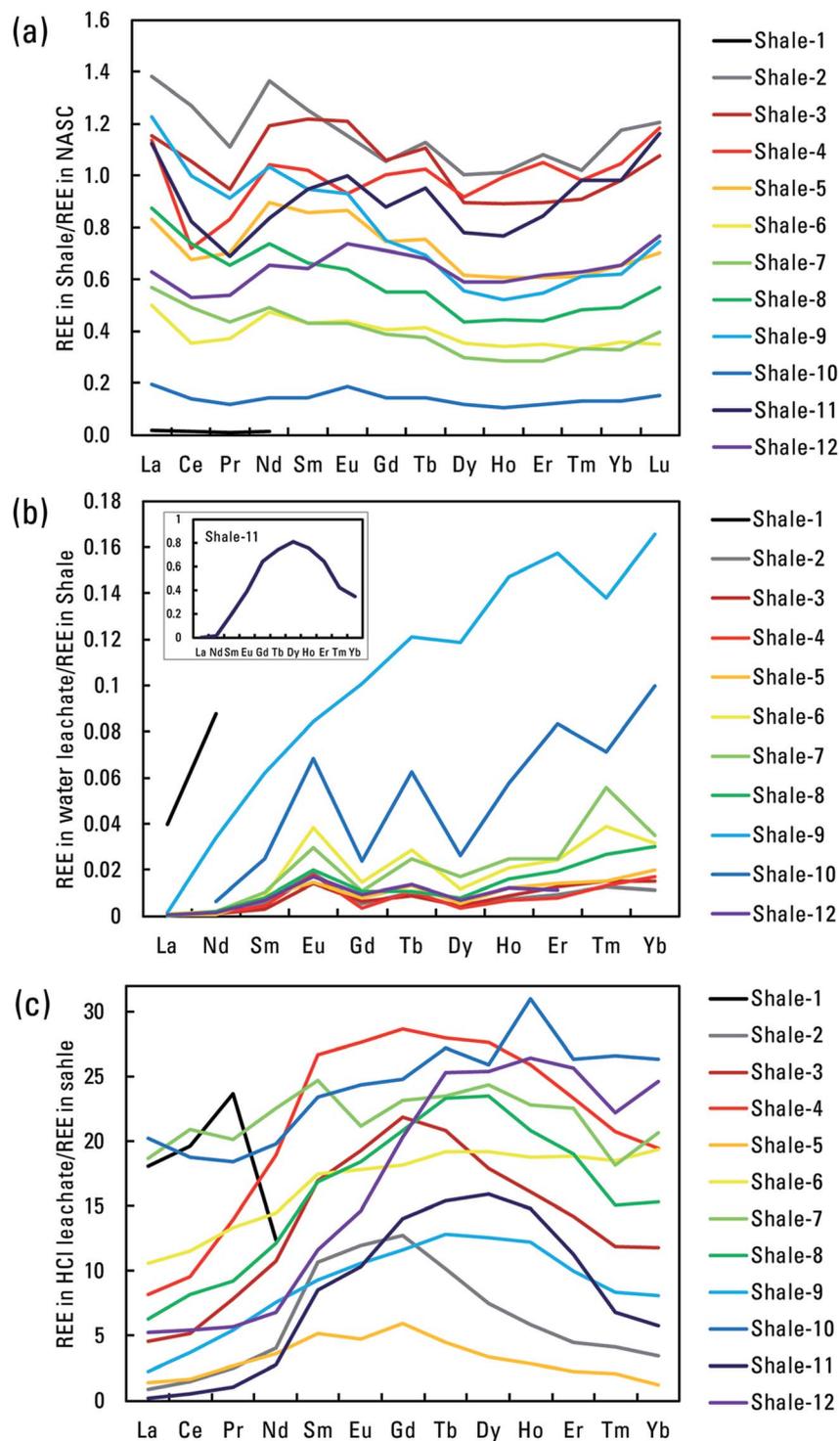This journal is © The Royal Society of Chemistry 2021

Fig. 9 Patterns of rare earth elements (REEs) in study materials: (a) REE concentrations in bulk shales normalized to the North American shale composite (NASC),[55] (b) REE concentrations in water leachates normalized to bulk shales, (c) REE concentrations in HCl leachates normalized to bulk shales. Ratios are dimensionless.

Another set of PCAs (Fig. 10) provided better insights into how the leachate compositions compared to produced waters than the simple concentration plots of Fig. 3. Brine and HCl shale leachate compositions were compared to produced waters compositions from the PWGD. Limited trace element data in the PWGD and the necessity for each sample included to have a concentration value for each element substantially narrowed the number of PWGD samples that could be included in the analyses. Ultimately, only conventional produced waters from various formations along the Texas Gulf Coast, shale gas waters
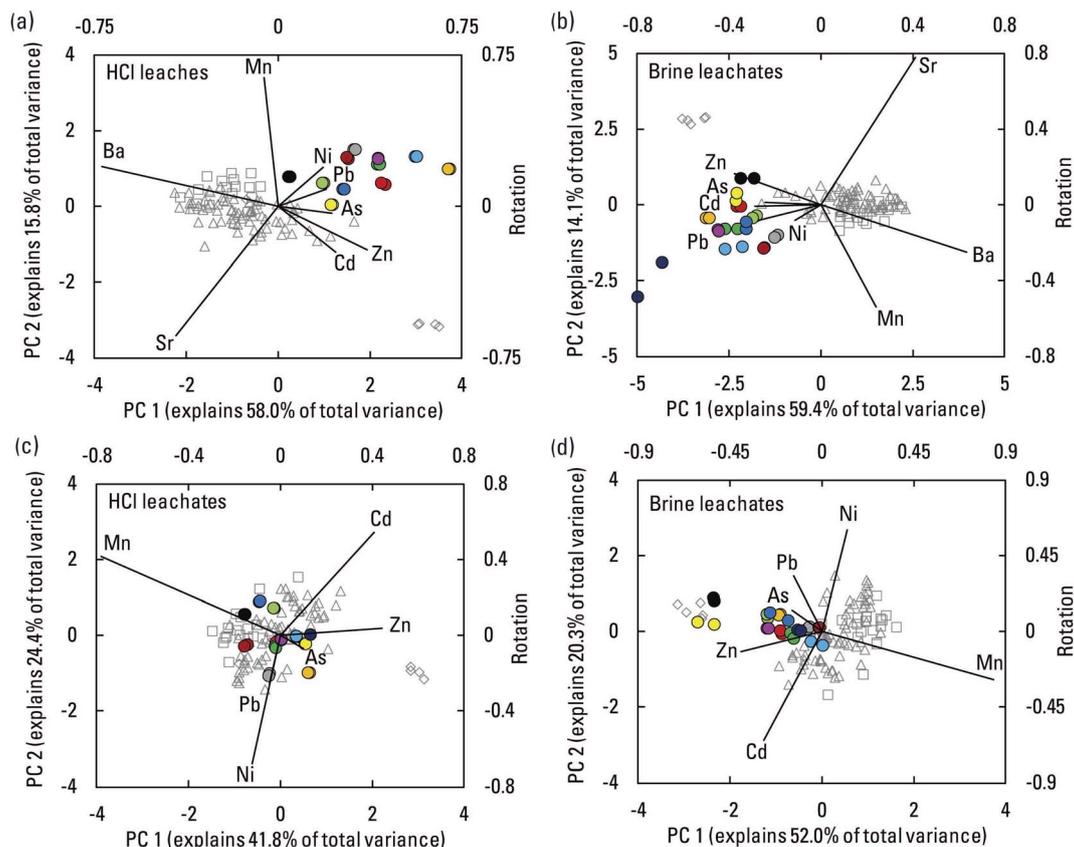
This journal is © The Royal Society of Chemistry 2021

Environ. Sci.: Processes Impacts, 2021, **23**, 1198–1219 | **1211**

Fig. 10 Biplots of results from principal component analysis of centered log ratio transformed compositions of the leachates and waters from the USGS Produced Waters Geochemical Database (PWGD; v2.3).[34] The PWGD samples include conventional produced waters from various formations along the Texas Gulf Coast, (open squares, $n = 18$), shale gas waters from the Marcellus shale (open triangles, $n = 66$), and tight oil produced waters from the Bakken formation (open diamonds, $n = 5$). Leachate sample points were colored as in Fig. 5. The produced water samples were included based upon availability of data for all included elements. Analyses (a) and (b) included As, Cd, Mn, Ni, Pb and Zn plus the alkaline earth elements Sr and Ba. Analyses (c) and (d) do not include Sr and Ba.

from the Marcellus shale, and tight oil produced waters from the Bakken formation were included. For the two analyses where the alkaline earth elements Sr and Ba were included lower concentrations of those elements in the leachates compared to the produced waters cause each to occupy separate areas of the multiparameter space of the PCA (Fig. 10a and b). However, when the analyses were restricted to just As, Cd, Mn, Ni, Pb and Zn (Fig. 7c and d), the leachates generally fell in the middle of the produced water sample distribution and even overlapped. Such similarity between leachates and produced waters indicated that the laboratory experiments produced similar overall mobilization patterns for those elements as water–rock interaction processes in the subsurface. The similarity between the produced waters from the Marcellus shale and Texas Gulf Coast formations indicated that produced water compositions with regards to As, Cd, Mn, Ni, Pb, and Zn may vary relatively narrowly among some basins and host formations. Waters from the Bakken formation did plot away from the other data along the ray projected for Zn and away from the ray projected for Mn. High and low concentrations, respectively, of those elements seem to reflect a different geochemical fingerprint for produced water from the Bakken formation (Fig. 3).

3.5. Comparison of leachates from the Marcellus shale and produced waters

Trace element comparisons across multiple basins and shale leachates provided a broad perspective, and a narrower focus on a particular formation helped confirm many of those patterns. The two leachates for the Marcellus shale samples were compared to the abundant corresponding produced waters data in the PWGD. To confirm that PWGD data for the Marcellus shale were representative, data were compared to another compilation of produced waters from the Appalachian basin. Concentrations for Al, Fe, Mn, SO_4^{2-}, As, Ba, Cd, Cr, and Pb compared favorably although mean concentrations for Cu and Zn were higher in the PWDB,[66] possibly reflecting development in new areas with somewhat different produced waters characteristics. Many other studies have presented results from a variety of water–rock interaction experiments for the Marcellus shale, and these were also compared to present data, particularly the brine leachates.[22,23,30–33,45,56] In general, concentrations from leaching experiments overlapped with produced waters for Al, As, Mo, Pb, Sb, and Zn (Fig. 11) and additionally for Cu, P, and Ti based on the other studies.[30–33,56] The present brine leachates were slightly low in Cd, Cr, and Ni, but other
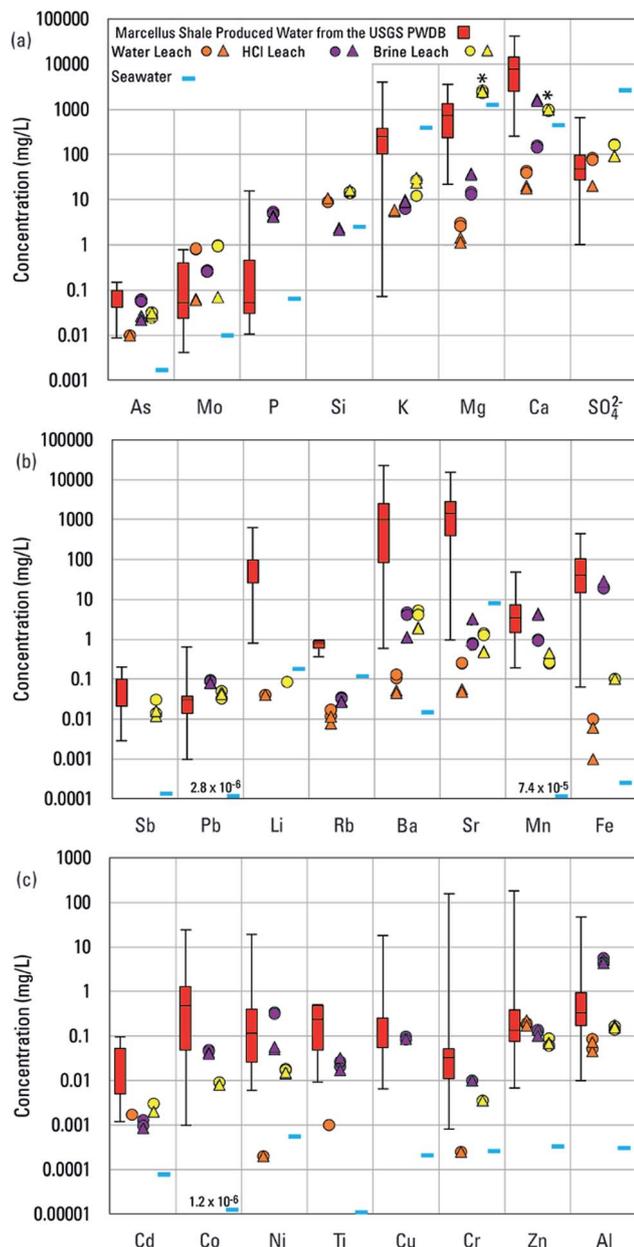
1212 | *Environ. Sci.: Processes Impacts*, 2021, **23**, 1198–1219

This journal is © The Royal Society of Chemistry 2021

Fig. 11 Concentrations of elements in produced waters from the Marcellus shale from the USGS Produced Waters Geochemical Database (v2.3)[34] plotted alongside concentrations in leachates from the two samples of Marcellus shale. Circles represent leachates from shale #2 (Onondaga County, New York) and triangles represent leachates from shale #3 (Genesee County, New York). Concentrations in modern seawater[51] are provided for reference. Asterisks indicate constituents (Ca and Mg) used to create the artificial brine prior to reaction with shale. Seawater concentrations less than the lower limit of the y-axis are printed on the figure.

studies compared more favorably.[30–32,56] Concentrations of Fe and Mn were low here and quite variable among the other experiments, depending strongly on pH and redox conditions.[22,23,30–33] Neither the present brine leachates nor any of the other experiments replicated produced waters concentrations for the Marcellus shale of Li, Sr, or Ba, a pattern that is consistent with the broader analysis (Fig. 3).[22,23,30–33,45,56]

3.6. Controls on Li, Sr, Ba in produced waters and shale leachates

The general failure of the present shale leaching experiments and those from other studies to reproduce produced water concentrations of Li, Sr, and Ba is notable because of the spectrum of pH, ionic strength, and other parameters the experiments represent (e.g. Fig. 4 and 6). Leachate Li, Sr, and Ba concentrations here were roughly $100\times$, $100\times$, and $10\times$ lower than in typical produced waters, respectively (Fig. 3). Low concentrations of Li in leachates might relate to certain mineral sources being slow to equilibrate, even under temperatures associated with hydrocarbon maturation used in many experiments.[31,67,68] Barium concentrations in water–rock interaction experiments can be limited by barite precipitation. As described in Section 3.2, the water and brine leachates here approached or exceeded saturation relative to barite, driven by SO_4^{2-} released by pyrite oxidation. Pyrite oxidation and barite saturation are common occurrences in shale leaching experiments, and Ba concentrations are always greater in experiments that exclude oxygen.[23,25,26,30,45,56,69] However, barite saturation also influences Ba concentrations in produced waters, as seen in the PWGD (Fig. S8†). Maximum Ba concentrations decline about $10\times$ between 100 and 1000 mg L^{-1} SO_4^{2-}, and about $100\times$ for SO_4^{2-} between 1000 and 10 000 mg L^{-1} SO_4^{2-}. Additionally, the HCl leachates were undersaturated relative to barite and yet still did not match typical concentrations of Ba in produced waters, although their leaching durations were short (1.5 h) (Fig. 3).

Insight into water–rock interaction and sources of the alkali and alkali earth metals is commonly sought by examining their ratios in fluids. Here, Li, Sr, and Ba are ratioed to Ca in leachates and produced waters, and additional insight is sought by comparison to ratios in seawater and evaporated seawater.[51,70] Ratios of Li/Ca in the water leachates generally overlap with produced waters but the other two leachate types show less overlap (Fig. 12). However, none of the leachates approached typical produced water Li concentrations (Fig. 3), and although evaporation of seawater drives Li/Ca ratios higher, this is driven partly by increases of Li with evaporation and partly by loss of Ca from solution at higher salinities. Ratios of Sr/Ca and Ba/Ca in the leachates showed slightly greater overlap with produced waters in some cases, though Sr and Ba concentrations did not (Fig. 3 and 12). As with Li/Ca, seawater evaporation drives Sr/Ca and Ba/Ca higher, but at the higher salinities, loss of Ca is a strong influence.

Isotopic studies have sought to understand the origins of Li, Sr, and Ba in Marcellus shale produced waters and how they relate to water–rock interaction. Lithium isotope ratios in Marcellus shale produced waters have values intermediate between seawater and those extracted via experiments with shale, but fractionations, systematics, and potential sources related to water–rock interaction are complex.[68,71] However, sources of elevated Li in produced waters from the Marcellus shale have been ascribed to diagenetic interactions with aluminosilicates in volcanogenic layers.[68] Such layers would not be present in all U.S. basins though, and Li concentrations and Li/Ca ratios are also elevated in other settings (Fig. 3 and 12).
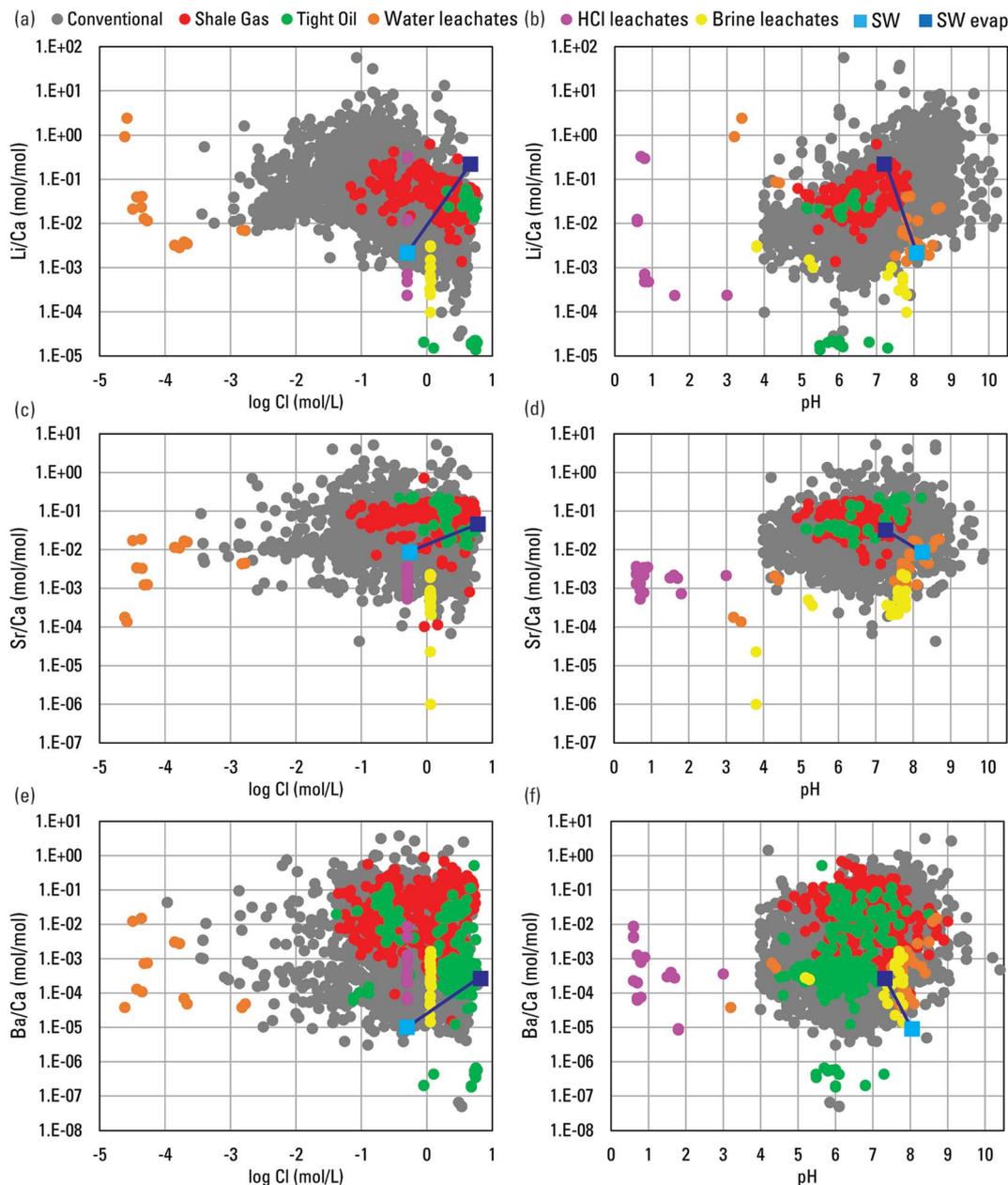
This journal is © The Royal Society of Chemistry 2021

Environ. Sci.: Processes Impacts, 2021, **23**, 1198–1219 | **1213**

Fig. 12 Scatterplots of molar Li/Ca ratios *versus* log Cl (a) and pH (b), Sr/Ca ratios *versus* log Cl (c) and pH (d), and Ba/Ca ratios *versus* log Cl (e) and pH (f) for waters from the from the USGS Produced Waters Geochemical Database (v2.3)[34] and water, HCl, and artificial brine leachates of shale. Modern seawater (SW) and evaporated seawater (SW evap.) are plotted for reference.[51,70]

Strontium isotope ratios in produced waters from the Marcellus shale have also posed a puzzle, being enriched in radiogenic Sr relative to carbonate sources in rock though sometimes similar to the exchangeable component.[59,71] Diagenetic interactions with aluminosilicates have been suggested as sources of the Sr with enriched isotope ratios.[59] Barium isotopes have helped confirm that dissolution from drilling mud is not a substantial source of Ba to produced waters from the Marcellus shale, but values in produced waters are also not entirely explained by exchangeable or carbonate sources in the shale.[72,73] All of these isotopic studies point toward contributions of Li, Sr, and Ba

from sources and processes related to diagenesis rather than water–rock interactions on shorter time scales.

Certain laboratory experiments with Marcellus shale have generated Li/Ca, Sr/Ca, and Ba/Ca ratios relatively close to the respective median values in produced waters from the Marcellus shale (4.4×10^{-2}, 8.7×10^{-2}, 5.5×10^{-2}, respectively) in the PWGD. Details of these experiments provide additional insight into drivers of the relatively high concentrations of these elements in produced waters. A study targeting water soluble and ion-exchangeable fractions on dry-drilled core material using 60 mL g^{-1} fluid-rock ratios yielded median 2.3×10^{-2} and 5.5×10^{-3} ratios for Sr/Ca and 1.2×10^{-2} and 5.5×10^{-2} ratios

for Ba/Ca, respectively.[59] A study that leached shale with NaCl brine under reducing conditions yielded a Ba/Ca ratio of 1.9×10^{-2} in solution, aided by absence of pyrite oxidation that kept SO_4^{2-} to 12 mg L^{-1}, but the Sr/Ca ratio was only 7.7×10^{-3}, possibly due to the 50 mL g^{-1} water–rock ratios.[45] A study specifically targeting brine trapped in pores and capillary water using 20 mL g^{-1} water–rock ratios yielded ratios of 9.6×10^{-3} for Sr/Ca and 6.2×10^{-3} for Ba/Ca. A time-series study using chips from slabbed core and 10 mL g^{-1} water–rock ratios with various strengths of artificial brines yielded median ratios of 1.2×10^{-2} for Li/Ca, 1.0×10^{-2} for Sr/Ca, but the median Ba/Ca ratio of 7.7×10^{-4} may have been limited by barite precipitation driven by pyrite oxidation.[31] Importantly, the Li/Ca ratios initially rose and then declined over time as Li concentrations appeared to approach asymptote, as if a finite pool of labile Li had been mobilized, like the isotopically distinct Li that can be desorbed from clays and organic matter in the Marcellus shale.[74]

All these results indicate that a combination of precipitated salts and brines in low permeability pore space, and ion-exchange sites equilibrated with such brines are the likely source for elevated concentrations of Li, Sr, and Ba in produced waters and their elevated ratios relative to Ca. That concept is well-established for the Marcellus shale, and the overlap with other produced waters (Fig. 12) indicates similar effects in other settings.[75,76] Comparison of conventional and unconventional water data from the PWGD for the same formations point towards additional pools of Li and Sr that are tapped by hydraulically fracturing the rock (Fig. 1). Tight oil waters from the Wolfcamp shale had a higher median Sr/Ca ratio of 6.6×10^{-2} ($n = 14$) compared to conventional waters with a median ratio of 1.1×10^{-2} ($n = 31$). Tight oil waters from the Bakken formation had a higher median Sr/Ca of 3.1×10^{-2} ($n = 33$) compared to a value from a conventional water of 2.5×10^{-3} ($n = 1$). The median Li/Ca ratio of tight oil waters from the Bakken formation 2.1×10^{-2} ($n = 33$) was also greater than that of conventional waters 6.3×10^{-3} ($n = 3$).

The likely reasons that laboratory leaching experiments cannot replicate produced waters concentrations and element ratios for Li, Sr, and Ca are several. First, brines in shale pores may be drawn out of drilled material as the exterior dries, whether obtained by wet- or dry-drilling methods. Rinsing of rock material (as was done here) and other handling can remove the migrated salts prior to extraction. Second, such pools of relatively labile elements can be small relative to sources in carbonates in many shales, and dissolution of carbonates helps mask dilution of the smaller pools. Finally, the water–rock ratios necessary in laboratory experiments to obtain sufficient sample volume for analysis are drastically different than those in the subsurface.

The water–rock ratios used here were 20 mL g^{-1} for the water and brine leachates and 16 mL g^{-1} for the HCl leachates. Similar experiments have used ratios of 4–1000 mL g^{-1}.[23,25–27,30–33,45,56,57] In contrast, water–rock ratios in the subsurface are lower by 3 or 4 orders of magnitude. Potential maximum water–rock ratios of 40 shales from the United States were calculated by dividing paired measurements of average

total porosity (median 11.2%, range 0.6–35.8%) by average dry bulk density (median 2.4 g cm^{-3}, range 1.56–2.81 g cm^{-3})[77] to yield a median value of 0.05 (range 0.003–0.23). Physically based estimates of water-connected porosity for the Marcellus shale are 0.01 (unweathered) and 0.06 (weathered) and chemically derived, water–rock ratios range from 0.007–0.04.[45] Small pools of Li, Sr, and Ba mobilized in part from salts, brines, and ion-exchange pools affected by diagenetic processes over geologic time scales would be substantially diluted by laboratory leachates compared to produced waters from unconventional resources. The migratory nature of waters derived from conventional resources mean that rock porosity may be less relevant that the volume of rock through which the waters have migrated. Proportionately small volumes of water reacting with large volumes of rock than contain relatively small fractions of labile elements seems to be a crucial factor for understanding the systematics of Li, Sr, and Ba in the subsurface and studying those systematics in the laboratory.

4. Conclusions

Major and trace element concentration data from the PWGD were summarized to gain perspective on typical concentrations and how they compare across hydrocarbon produced waters well types from the United States. Produced waters concentrations were compared to concentrations in seawater and in experimental leachates from U.S. energy-related shales to gain insights into the influence of water–rock interactions on produced waters compositions. Inheritance from paleo-seawater, bitterns, and evaporites largely explained the produced water concentrations of many major elements. Low concentrations of many trace elements in seawater indicated that in produced waters these trace elements are sourced from water–rock interaction with sedimentary rocks, particularly shales. Comparisons of produced waters compositions and shale leachates indicated that water–rock interactions influenced by pH and ionic strength can explain concentrations for some elements (Al, As, Cd, Co, Cu, Mn, Mo, Ni, Pb, Sb, Si, and Zn). Low pH solutions enhanced mobilization of MREEs relative to proportions in shales, but available produced water data on REEs are insufficient to confirm a similar environmental effect. Produced water concentrations of Li, Sr, and Ba are not replicated by simple, separate low pH or high ionic strength experiments. This study and others indicate that experimental failure to match produced water concentrations of Li, Sr, and Ba or their ratios to Ca stems from their predominant sourcing from small pools of salts, brines, and ion-exchange sites affected by diagenetic processes that become diluted and masked by other water–rock interaction processes at the greater water–rock ratios necessitated in the laboratory. Similarities in Li, Sr, and Ba concentrations and ratios to Ca across basins and produced waters well types indicates analogous effects in a variety of settings.

Conflicts of interest

There are no conflicts of interest to declare.

This journal is © The Royal Society of Chemistry 2021

Environ. Sci.: Processes Impacts, 2021, **23**, 1198–1219 | **1215**

Acknowledgements

References

1 J. Neff, K. Lee and E. M. DeBlois, in *Produced Water*, Springer, New York, NY, 2011, pp. 3–54.

2 B. E. Fontenot, L. R. Hunt, Z. L. Hildenbrand, D. D. Carlton Jr, H. Oka, J. L. Walton, D. Hopkins, A. Osorio, B. Bjorndal, Q. H. Hu and K. A. Schug, An evaluation of water quality in private drinking water wells near natural gas extraction sites in the Barnett Shale Formation, *Environ. Sci. Technol.*, 2013, **47**, 10032–10040, DOI: 10.11021/es4011724.

3 A. Vengosh, R. B. Jackson, N. Warner, T. H. Darrah and A. J. Kondash, A critical review of the risks to water resources from unconventional gas development and hydraulic fracturing in the United States, *Environ. Sci. Technol.*, 2014, **48**, 8334–8348, DOI: 10.1021/es405118y.

4 A. Vengosh, N. Warner, R. Jackson and T. Darrah, The effects of shale gas exploration and hydraulic fracturing on the quality of water resources in the United States, *Procedia Earth Planet. Sci.*, 2013, **7**, 863–866, DOI: 10.1016/j.proeps.2013.1003.1213.

5 R. D. Vidic, S. L. Brantley, J. M. Vandenbossche, D. Yoxtheimer and J. D. Abad, Impact of shale gas development on regional water quality, *Science*, 2013, **340**, 1235009, DOI: 10.1231126/science.1235009.

6 S. S. Haines, T. A. Cook, J. N. Thamke, K. W. Davis, A. J. Long, R. W. Healy, S. J. Hawkins and M. A. Engle, A framework for assessing water and proppant use and flowback water extraction associated with development of continuous petroleum resources, *U.S. Geological Survey Fact Sheet*, 2014, vol. 2014–3010, p. 6, DOI: 10.3133/fs20143010.

7 B. R. Scanlon, R. C. Reedy and J.-P. Nicot, Comparison of water use for hydraulic fracturing for unconventional oil and gas *versus* conventional oil, *Environ. Sci. Technol.*, 2014, **48**, 310–320, DOI: 10.1021/es502506v.

8 C. T. Montgomery and M. B. Smith, Hydraulic fracturing: History of an enduring technology, *J. Pet. Technol.*, 2010, **62**, 26–40, DOI: 10.2118/1210-0026-JPT.

9 R. LeBas, P. Lord, D. Luna and T. Shahan, Development and use of high-TDS recycled produced water for crosslinked-gel-based hydraulic fracturing, *Proceedings of the SPE Hydraulic Fracturing Technology Conference*, Woodlands, TX, 4–6 February, 2013, p. 9, DOI: 10.2118/163824-MS.

10 T. J. Gallegos, C. R. Bern, J. E. Birdwell, S. S. Haines and M. Engle, in *Food, Energy, and Water: The Chemistry Connection*, Elsevier, 2015, pp. 183–215, DOI: 10.1016/B1978-1010-1012-800211-800217.800007-800217.

11 B. R. Scanlon, R. C. Reedy, P. Xu, M. Engle, J. P. Nicot, D. Yoxtheimer, Q. Yang and S. Ikonnikova, Can we beneficially reuse produced water from oil and gas extraction in the U.S.?, *Sci. Total Environ.*, 2020, **717**, 137085, DOI: 10.1016/j.scitotenv.2020.137085.

12 M. A. Al-Ghouti, M. A. Al-Kaabi, M. Y. Ashfaq and D. Da'na, Produced water characteristics, treatment and reuse: A review, *J. Water Process.*, 2019, **28**, 222–239, DOI: 10.1016/j.jwpe.2019.1002.1001.

13 D. T. Long and E. E. Angino, The mobilization of selected trace metals from shales by aqueous solutions: Effects of temperature and ionic strength, *Econ. Geol.*, 1982, **77**, 646–652, DOI: 10.2113/gsecongeo.2177.2113.2646.

14 Y. K. Kharaka and J. S. Hanor, in *Treatise on Geochemistry*, 2nd edn, 2014, pp. 471–515, DOI: 10.1016/B1978-1010-1008-095975-095977.000516-095977.

15 P. A. Abanda and R. E. Hannigan, Effect of diagenesis on trace element partitioning in shales, *Chem. Geol.*, 2006, **230**, 42–59, DOI: 10.1016/j.chemgeo.2005.1011.1011.

16 J. D. Rimstidt, J. A. Chermak and M. E. Schreiber, Processes that control mineral and element abundances in shales, *Earth-Sci. Rev.*, 2017, **171**, 383–399, DOI: 10.1016/j.earscirev.2017.1006.1010.

17 Variations in chloride as a driving force in siliciclastic diagenesis, ed. L. J. Crossey, R. Loucks, M. W. Totten, *Siliciclastic Diagenesis and Fluid Flow: Concepts and Applications, Special Publication 55*, SEPM Society for Sedimentary Geology, 1996, pp. 3–12.

18 E. Barbot, N. S. Vidic, K. B. Gregory and R. D. Vidic, Spatial and temporal correlation of water quality parameters of produced waters from Devonian-age shale following hydraulic fracturing, *Environ. Sci. Technol.*, 2013, **47**, 2562–2569, DOI: 10.1021/es304638h.

19 E. L. Rowan, M. A. Engle, T. F. Kraemer, K. T. Schroeder, R. W. Hammack and M. W. Doughten, Geochemical and isotopic evolution of water produced from Middle Devonian Marcellus shale gas wells, Appalachian basin, Pennsylvania, *AAPG Bull.*, 2015, **99**, 181–206, DOI: 10.1306/07071413146.

20 L. O. Haluszczak, A. W. Rose and L. R. Kump, Geochemical evaluation of flowback brine from Marcellus gas wells in Pennsylvania, USA, *Appl. Geochem.*, 2013, **28**, 55–61, DOI: 10.1016/j.apgeochem.2012.1010.1002.

21 Y. K. Kharaka, K. D. Gans, E. L. Rowan, J. J. Thordsen, C. Conaway, M. S. Blondes and M. Engle, in *Shale: Subsurface Science and Engineering, Geophysical Monograph 245*, ed. T. Dewers, J. Heath and M. Sánchez, John Wiley & Sons, Inc., 2020, pp. 27–43.

22 M. Ali and B. Hascakir, Water-rock interaction for Eagle Ford, Marcellus, Green River, and Barnett Shale samples and implications for hydraulic-fracturing-fluid engineering, *SPE J.*, 2015, **22**, 162–171, DOI: 10.2118/177304-PA.

1216 | *Environ. Sci.: Processes Impacts*, 2021, **23**, 1198–1219

This journal is © The Royal Society of Chemistry 2021

23 J. Pilewski, S. Sharma, V. Agrawal, J. A. Hakala and M. Y. Stuckman, Effect of maturity and mineralogy on fluid-rock reactions in the Marcellus Shale, *Environ. Sci.: Processes Impacts*, 2019, **21**, 845–855, DOI: 10.1039/C1038EM00452H.

24 K. Piszcz-Karaś, J. Łuczak and J. Hupka, Release of selected chemical elements from shale drill cuttings to aqueous solutions of different pH, *Appl. Geochem.*, 2016, **72**, 136–145, DOI: 10.1016/j.apgeochem.2016.1007.1006.

25 L. Wang, J. D. Fortner and D. E. Giammar, Impact of water chemistry on element mobilization from Eagle Ford Shale, *Environ. Eng. Sci.*, 2015, **32**, 310–320, DOI: 10.1089/ees.2014.0342.

26 L. Wang, S. Burns, D. E. Giammar and J. D. Fortner, Element mobilization from Bakken shales as a function of water chemistry, *Chemosphere*, 2016, **149**, 286–293, DOI: 10.1016/j.chemosphere.2016.1001.1107.

27 F. D. Wilke, A. Vieth-Hillebrand, R. Naumann, J. Erzinger and B. Horsfield, Induced mobility of inorganic and organic solutes from black shales using water extraction: Implications for shale gas exploitation, *Appl. Geochem.*, 2015, **63**, 158–168, DOI: 10.1016/j.apgeochem.2015.1007.1008.

28 A. Zolfaghari, J. Holyk, Y. Tang, H. Dehghanpour and D. Bearinger, Flowback chemical analysis: An interplay of shale-water interactions, *SPE Asia Pacific Unconventional Resources Conference and Exhibition*, Brisbane, Australia, 2015.

29 S. Sharma, V. Agrawal, R. N. Akondi, Y. Wang and A. Hakala, Understanding controls on the geochemistry of hydrocarbon produced waters from different basins across the US, *Environ. Sci.: Processes Impacts*, 2021, **23**, 28–47, DOI: 10.1039/d1030em00388c.

30 V. Marcon, C. Joseph, K. E. Carter, S. W. Hedges, C. L. Lopano, G. D. Guthrie and J. A. Hakala, Experimental insights into geochemical changes in hydraulically fractured Marcellus Shale, *Appl. Geochem.*, 2017, **76**, 36–50, DOI: 10.1016/j.apgeochem.2016.1011.1005.

31 J. Lu, P. J. Mickler, J.-P. Nicot, W. Choi, W. L. Esch and R. Darvari, Geochemical interactions of shale and brine in autoclave experiments—Understanding mineral reactions during hydraulic fracturing of Marcellus and Eagle Ford Shales, *AAPG Bull.*, 2017, **101**, 1567–1597, DOI: 10.1306/11101616026.

32 A. L. Harrison, A. D. Jew, M. K. Dustin, D. L. Thomas, C. M. Joe-Wong, J. R. Bargar, N. Johnson, G. E. Brown Jr. and K. Maher, Element release and reaction-induced porosity alteration during shale-hydraulic fracturing fluid interactions, *Appl. Geochem.*, 2017, **82**, 47–62, DOI: 10.1016/j.apgeochem.2017.1005.1001.

33 T. L. Tasker, P. K. Piotrowski, F. L. Dorman and W. D. Burgos, Metal associations in Marcellus Shale and fate of synthetic hydraulic fracturing fluids reacted at high pressure and temperature, *Environ. Eng. Sci.*, 2016, **33**, 753–765, DOI: 10.1089/ees.2015.0605.

34 M. S. Blondes, K. D. Gans, M. A. Engle, Y. K. Kharaka, M. E. Reidy, V. Saraswathula, J. J. Thordsen, E. L. Rowan and E. A. Morrissey, *U.S. Geological Survey National Produced Waters Geochemical Database (ver2.3, January 2018)*, 2018, U.S. Geological Survey data release, DOI: 10.5066/F5067J5964W5068.

35 S. M. McLennan, Relationships between the trace element composition of sedimentary rocks and upper continental crust, *Geochem., Geophys., Geosyst.*, 2001, **2**, 24, DOI: 10.1029/2000GC000109.

36 J. A. Chermak and M. E. Schreiber, Mineralogy and trace element geochemistry of gas shales in the United States: Environmental implications, *Int. J. Coal Geol.*, 2014, **126**, 32–44, DOI: 10.1016/j.coal.2013.1012.1005.

37 M. Croke, C. R. Bern, J. E. Birdwell, A. M. Jubb, M. Adams and J. Chenault, Results of leaching experiments on 12 energy-related shales from the United States, U.S. Geological Survey data release, 2020, DOI: DOI: 10.5066/P5098GUULU.

38 C. Nye, G. Neupane, S. Quillinan and T. McLing, in *Assessing rare earth element concentrations in geothermal and oil and gas produced waters: A potential domestic source of strategic mineral commodities*, 2018, Final Report to U.S. Department of Energy, Geothermal Technologies Office DE-EE0007603, pp. 0007647–0007665.

39 L. Tian, H. Chang, P. Tang, T. Li, X. Zhang, S. Liu, Q. He, T. Wang, J. Yang, Y. Bai, R. D. Vidic, J. C. Crittenden and B. Liu, Rare Earth Elements Occurrence and Economical Recovery Strategy from Shale Gas Wastewater in the Sichuan Basin, China, *ACS Sustainable Chem. Eng.*, 2020, **8**, 11914–11920, DOI: 10.11021/acssuschemeng.11910c04971.

40 B. Hitchon and M. Brulotte, Culling criteria for "standard" formation water analysis, *Appl. Geochem.*, 1994, **9**, 637–645, DOI: 10.1016/0883-2927(1094)90024-90028.

41 J. C. Osmond, in *Hydrocarbon and mineral resources of the Unita Basin, Utah and Colorado: Utah Geological Association Guidebook No. 20*, ed. T. D. Fouch, V. F. Nuccio and T. C. Chidsey, 1992, pp. 143–163.

42 J. E. Birdwell, M. D. Vanden Berg, R. C. Johnson, T. J. Mercier, A. R. Boehlke and M. E. Brownfield, in *Hydrocarbon Source Rocks in Unconventional Plays, Rocky Mountain Region*, ed. M. P. Dolan, D. H. Higley and P. G. Lillis, Rocky Mountain Association of Geologists, Denver, Colorado, 2016, pp. 352–378.

43 R. C. Johnson, J. E. Birdwell, T. J. Mercier and M. E. Brownfield, Geology of tight oil and potential tight oil reservoirs in the lower part of the Green River Formation, Uinta, Piceance, and Greater Green River Basins, Utah, Colorado, and Wyoming, *U.S. Geological Survey, Scientific Investigations Report*, 2016, vol. 5008, p. 63, DOI: 10.3133/sir20165008.

44 J. E. Birdwell, R. C. Johnson and M. E. Brownfield, Distribution of mineral phases in the Eocene Green River Formation, Piceance Basin, Colorado – Implications for the evolution of Lake Uinta, *Mt. Geol.*, 2019, **56**, 73–141, DOI: 10.31582/rmag.mg.31556.31582.31573.

45 D. Renock, J. D. Landis and M. Sharma, Reductive weathering of black shale and release of barium during

This journal is © The Royal Society of Chemistry 2021

Environ. Sci.: Processes Impacts, 2021, **23**, 1198–1219 | 1217

hydraulic fracturing, *Appl. Geochem.*, 2016, **65**, 73–86, DOI: 10.1016/j.apgeochem.2015.1011.1001.

46 M. A. Engle, F. R. Reyes, M. S. Varonka, W. H. Orem, L. Ma, A. J. Ianno, T. M. Schell, P. Xu and K. C. Carroll, Geochemistry of formation waters from the Wolfcamp and "Cline" shales: Insights into brine origin, reservoir connectivity, and fluid flow in the Permian Basin, USA, *Chem. Geol.*, 2016, **425**, 76–92, DOI: 10.1016/j.chemgeo.2016.1001.1025.

47 R Core Team, *R: A language and environment for statistical computing*, R Foundation for Statistical Computing, Vienna, Austria, 2020, https://www.R-project.org/.

48 C. R. Bern, K. Walton-Day and D. Naftz, Improved enrichment factor calculations through principal component analysis: Examples from soils near breccia pipe uranium mines, *Arizona, USA, Environmental Pollution*, 2019, vol. 248, pp. 90–100, DOI: 10.1016/j.envpol.2019.1001.1122.

49 C. Reimann, P. Filzmoser, R. G. Garrett and R. Dutter, *Statistical Data Analysis Explained: Applied Environmental Statistics with R*, John Wiley & Sons, Ltd, New York, 2008.

50 S. B. Gaswirth, Structure Contour and Isopach Maps of the Wolfcamp Shale and Bone Spring Formation of the Delaware Basin, Permian Basin Province, New Mexico and Texas, *U.S. Geological Survey, Open-File Report*, 2020, vol. 1126, p. 37, DOI: 10.3133/ofr20201126.

51 Y.-H. Li, Distribution patterns of the elements in the ocean: A synthesis, *Geochim. Cosmochim. Acta*, 1991, **55**, 3223–3240, DOI: 10.1016/0016-7037(3291)90485-N.

52 J. S. Hanor, Physical and chemical controls on the composition of waters in sedimentary basins, *Mar. Petrol. Geol.*, 1994, **11**, 31–45, DOI: 10.1016/0264-8172(1094)90007-90008.

53 J. S. Hanor, Reactive transport involving rock-buffered fluids of varying salinity, *Geochim. Cosmochim. Acta*, 2001, **65**, 3721–3732, DOI: 10.1016/S0016-7037(3701)00703-00707.

54 J. S. Hanor, in *Carbonate-hosted Lead–Zinc Deposits*, ed. D. F. Sangster, SEG Special Publication, 1996, vol. 4, pp. 483–500.

55 L. P. Gromet, L. A. Haskin, R. L. Korotev and R. F. Dymek, The "North American shale composite": Its compilation, major and trace element characteristics, *Geochim. Cosmochim. Acta*, 1984, **48**, 2469–2482, DOI: 10.1016/0016-7037(2484)90298-90299.

56 N. Mehta and B. D. Kocar, Geochemical conditions conducive for retention of trace elements and radionuclides during shale–fluid interactions, *Environ. Sci.: Processes Impacts*, 2019, **21**, 1764–1776, DOI: 10.1039/C1769EM00244H.

57 J. D. Johnson and J. R. Graney, Fingerprinting Marcellus Shale waste products from Pb isotope and trace metal perspectives, *Appl. Geochem.*, 2015, **60**, 104–115, DOI: 10.1016/j.apgeochem.2015.1004.1021.

58 U. Lavergren, M. E. Åström, B. Bergbäck and H. Holmström, Mobility of trace elements in black shale assessed by leaching tests and sequential chemical extraction, *Geochem.: Explor., Environ., Anal.*, 2009, **9**, 71–79, DOI: 10.1144/1467-7873/1108-1188.

59 B. W. Stewart, E. C. Chapman, R. C. Capo, J. D. Johnson, J. R. Graney, C. S. Kirby and K. T. Schroeder, Origin of brines, salts and carbonate from shales of the Marcellus Formation: Evidence from geochemical and Sr isotope study of sequentially extracted fluids, *Appl. Geochem.*, 2015, **60**, 78–88, DOI: 10.1016/j.apgeochem.2015.1001.1004.

60 D. Parkhurst and C. Appelo, User's guide to PHREEQC (Version 2) — A computer program for speciation, batch-reaction, one-dimensional transport, and inverse geochemical calculations, *U.S. Geol Survey Water-Resour Inv Rep 99–4259*, 1999, p. 310.

61 P. A. Abanda and R. E. Hannigan, Effect of diagenesis on trace element partitioning in shales, *Chem. Geol.*, 2006, **230**, 42–59, DOI: 10.1016/j.chemgeo.2005.1011.1011.

62 C. W. Noak, J. C. Jain, J. Stegmeier, J. A. Hakala and A. K. Karamalidis, Rare earth element geochemistry of outcrop and core samples from the Marcellus Shale, *Geochem. Trans.*, 2015, **16**, 6, DOI: 10.1186/s12932-12015-10022-12934.

63 L. Ma, L. Jin and S. L. Brantley, How mineralogy and slope aspect affect REE release and fractionation during shale weathering in the Susquehanna/Shale Hills Critical Zone Observatory, *Chem. Geol.*, 2011, **290**, 31–49, DOI: 10.1016/j.chemgeo.2011.1008.1013.

64 I. L. R. Wallrich, B. W. Stewart, R. C. Capo, B. C. Hedin and T. T. Phan, Neodymium isotopes track sources of rare earth elements in acidic mine waters, *Geochim. Cosmochim. Acta*, 2020, **269**, 465–483, DOI: 10.1016/j.gca.2019.1010.1004.

65 S. Chaudhuri and N. Clauer, Strontium isotopic compositions and potassium and rubidium contents of formation waters in sedimentary basins: Clues to the origin of the solutes, *Geochim. Cosmochim. Acta*, 1993, **57**, 429–437, DOI: 10.1016/0016-7037(1093)90441-X.

66 N. Abualfaraj, P. L. Gurian and M. S. Olson, Characterization of Marcellus shale flowback water, *Environ. Eng. Sci.*, 2014, **31**, 514–524, DOI: 10.1089/ees.2014.0001.

67 Y. K. Kharaka and R. H. Mariner, in *Thermal History of Sedimentary Basins*, ed. N. D. Naeser and T. H. McCulloh, Springer, New York, 1989, pp. 99–117, DOI: 10.1007/1978-1001-4612-3492-1000_1006.

68 T. T. Phan, R. C. Capo, B. W. Stewart, G. L. Macpherson, E. L. Rowan and R. W. Hammack, Factors controlling Li concentration and isotopic composition in formation waters and host rocks of Marcellus Shale, *Appalachian Basin, Chemical Geology*, 2016, **420**, 162–179, DOI: 10.1016/j.chemgeo.2015.1011.1003.

69 F. Osselin, S. Saad, M. Nightingale, G. Hearn, A.-M. Desaulty, E. C. Gaucher, C. R. Clarkson, W. Kloppmann and B. Mayer, Geochemical and sulfate isotopic evolution of flowback and produced waters reveals water-rock interactions following hydraulic fracturing of a tight hydrocarbon reservoir, *Sci. Total Environ.*, 2019, **687**, 1389–1400, DOI: 10.1016/j.scitotenv.2019.1307.1066.

70 Y. O. Rosenberg, Z. Sade and J. Ganor, The precipitation of gypsum, celestine, and barite and coprecipitation of radium during seawater evaporation, *Geochim. Cosmochim. Acta*, 2018, **233**, 50–65, DOI: 10.1016/j.gca.2018.1004.1019.

1218 | *Environ. Sci.: Processes Impacts*, 2021, **23**, 1198–1219

This journal is © The Royal Society of Chemistry 2021

71 T. T. Phan, A. N. Vankeuren and J. A. Hakala, Role of water–rock interaction in the geochemical evolution of Marcellus Shale produced waters, *Int. J. Coal Geol.*, 2018, **191**, 95–111, DOI: 10.1016/j.coal.2018.1002.1014.

72 A. D. Jew, Q. Li, D. Cercone, K. Maher, G. E. Brown Jr and J. R. Bargar, Barium Sources in Hydraulic Fracturing Systems and Chemical Controls on Its Release Into Solution, *Unconventional Resources Technology Conference*, Houston, Texas, 2018, pp. 863–874, DOI: 10.15530/urtec-2018-2899671.

73 Z. G. Tieman, B. W. Stewart, R. C. Capo, T. T. Phan, C. L. Lopano and J. A. Hakala, Barium isotopes track the source of dissolved solids in produced water from the unconventional Marcellus Shale gas play, *Environ. Sci. Technol.*, 2020, **54**, 4275–4285, DOI: 10.1021/acs.est.4270c00102.

74 T. T. Phan, J. A. Hakala and S. Sharma, Application of isotopic and geochemical signals in unconventional oil and gas reservoir producedwaters toward characterizing *in situ* geochemical fluid-shale reactions, *Sci. Total Environ.*, 2020, **714**, DOI: 10.1016/j.scitotenv.2020.136867.

75 S. A. Welch, J. M. Sheets, R. A. Daly, A. Hanson, S. Sharma, T. Darrah, J. Olesik, A. Lutton, P. J. Mouser, K. C. Wrighton, M. J. Wilkins, T. Carr and D. R. Cole, Comparative geochemistry of flowback chemistry from the Utica/Point Pleasant and Marcellus formations, *Chem. Geol.*, 2021, **564**, 120041, DOI: 10.1016/j.chemgeo.2020.120041.

76 E. L. Rowan, M. A. Engle, T. F. Kraemer, K. T. Schroeder, R. W. Hammack and M. W. Doughten, Geochemical and isotopic evolution of water produced from Middle Devonian Marcellus shale gas wells, Appalachian basin, Pennsylvania, *AAPG Bull.*, 2015, **99**, 181–206, DOI: 10.1306/07071413146.

77 G. E. Manger, Porosity and bulk density of sedimentary rocks, *U.S. Geological Survey Bulletin*, 1963, 1144-E, p. 55, DOI: 10.3133/b1144E.

This journal is © The Royal Society of Chemistry 2021

Environ. Sci.: Processes Impacts, 2021, **23**, 1198–1219 | **1219**